August 2017

Design and Development of a Robot Guided Rehabilitation Scheme for Upper Extremity Rehabilitation

Md Assad-Uz-Zaman
University of Wisconsin-Milwaukee

DESIGN AND DEVELOPMENT OF A ROBOT GUIDED REHABILITATION SCHEME FOR UPPER EXTREMITY REHABILITATION

by

Md Assad-Uz-Zaman

A Thesis Submitted in

Partial Fulfillment of the

Requirements for the Degree of

Master of Science

in Engineering

at

University of Wisconsin-Milwaukee

August 2017

ABSTRACT

DESIGN AND DEVELOPMENT OF A ROBOT GUIDED REHABILITATION SCHEME FOR UPPER EXTREMITY REHABILITATION

by

Md Assad-Uz-Zaman

University of Wisconsin-Milwaukee, 2017
Under the Supervision of Professor Mohammad Habibur Rahman

To rehabilitate individuals with impaired upper-limb function, we have designed and developed a robot guided rehabilitation scheme. A humanoid robot, NAO was used for this purpose. NAO has 25 degrees of freedom. With its sensors and actuators, it can walk forward and backward, can sit down and stand up, can wave his hand, can speak to the audience, can feel the touch sensation, and can recognize the person he is meeting. All these qualities have made NAO a perfect coach to guide the subjects to perform rehabilitation exercises. To demonstrate rehabilitation exercises with NAO, a library of recommended rehabilitation exercises involving shoulder (i.e., abduction/adduction, vertical flexion/extension, and internal/external rotation), and elbow (i.e., flexion/extension) joint movements was formed in Choregraphe (graphical programming interface). In experiments, NAO was maneuvered to instruct and demonstrate the exercises from the NRL. A complex 'touch and play' game was also developed where NAO plays with the subject that represents a multi-joint movement's exercise. To develop the proposed tele-rehabilitation scheme, kinematic model of human upper-extremity was developed based modified Denavit-Hartenberg notations. A complete

geometric solution was developed to find a unique inverse kinematic solution of human upper-extremity from the Kinect data. In tele-rehabilitation scheme, a therapist can remotely tele-operate the NAO in real-time to instruct and demonstrate subjects different arm movement exercises. Kinect sensor was used in this scheme to get tele-operator's kinematics data. Experiments results reveals that NAO can be tele-operated successfully to instruct and demonstrate subjects to perform different arm movement exercises. A control algorithm was developed in MATLAB for the proposed robot guided supervised rehabilitation scheme. Experimental results show that the NAO and Kinect sensor can effectively be used to supervise and guide the subjects in performing active rehabilitation exercises for shoulder and elbow joint movements.

Key words: Arm impairment, Robot guided rehabilitation therapy, NAO, Choregraphe, Kinect, Rehabilitation, Tele-operation, Supervised rehabilitation scheme, Intelligent control, Kinematics

TABLE OF CONTENTS

LIST OF FIGURES

LIST OF TABLES

ACKNOWLEDGEMENTS

First and foremost, I would like to pay my gratitude to almighty ALLAH (SWT), who gives me the strength, courage and patience for completing this thesis work at last. I would like to acknowledge my advisor Dr. Mohammad Habibur Rahman for his immense support and guidance. Dr. Rahman recognized my potential to contribute to the rehabilitation robotics field. He has also served as a constant source of encouragement and counseling during the journey towards my MS. My committee members have been truly wonderful in their comments and creative ideas. I thank Dr. Yongjin Sung and Dr. Veysi Malkoc for serving on my thesis committee. I would also like to thank my lab mate Md Rasedul Islam, PhD Student at mechanical engineering department, who has been a ceaseless source of inspiration and motivation during this journey. A special thanks to my other lab-mates Rezwan, Mark, Chris, Liu, Fidel, Nick and Anna, for helping me and providing a supportive environment to work in.

I would like to thank Professor Dr. Mohammad Mashud for his support, encouragement and enlightenment throughout my life.

I want to convey my deepest gratitude to my father and mother for their endless struggle to bring me at this level and their encouragement. I also want to mention my gratitude to my father-in-law and mother-in-law for their believe and support for me.

Finally yet importantly, I like to mention my heartiest thanks to an integral part of my life, my wife Zannatul Ferdous Monika, for her enormous patience, continuous support and encouragement during this stressful time.

CHAPTER 1

INTRODUCTION

Upper extremity impairment is very common due to geriatric disorders and/or following a stroke or other conditions such as TBI, SCI, sports, falls, and traumatic injuries. According to the World Health Organization (WHO), a stroke is a sudden ischemic or hemorrhagic interruption in the blood flow supplying oxygen and nutrients to the brain tissue. This event results in brain cell death and consequently in partial loss of neurological function (World Health Organization 2010). The occurrence of strokes has been progressively increasing. Currently, according to CDC (Centers for Disease Control and Prevention), strokes are the fourth leading cause of mortality in the USA. The consequences of strokes extend further than patient mortality. The majority of stroke survivors live with long-term disabilities, leading to serious social and economic impacts: it is estimated that stroke and heart diseases cost more than $34 billion annually worldwide (Mozaffarian, Benjamin et al. 2015). These numbers will continue to rise as the *aging* population increases.

Rehabilitation programs are the main method to promote functional recovery in these individuals (Gresham, Alexander et al. 1997, Truelsen, Piechowski-Jozwiak et al. 2006). The Conventional therapeutic approach requires a long commitment by a therapist or clinician. Unfortunately, there is a consistent shortage of qualified physiotherapists/clinicians both in developing countries and in the developed countries as well. Beside this, the treatment duration is usually very long, requiring many hours of the therapist's time for each individual patient. On top of these facts, the number of such cases is constantly growing. Therefore, an alternative to the conventional treatments is essential.

To assist physically disabled individuals with impaired upper limb function, extensive research has been carried out in many branches of robotics, particularly on wearable robots e.g., exoskeletons (Rahman, Kiguchi et al. 2006, Garrec, Friconneau et al. 2008, Nef, Guidali et al. 2009). Although much progress has been made, we are still far from the desired achievement, as existing robots have not yet been able to restore body mobility or function.

Several hypotheses exist as to how upper extremity rehabilitation may be improved. Studies reveal that intensive and repetitive therapies significantly improve motor skill (Huang et al., 2009). Note that the passive rehabilitation therapy does not contribute in building muscle but does help to prevent contractures, increasing the range of motion and thus maintains and promotes mobility of the patients (Wang, 2011). Therefore, once resistance to passive arm movements in individuals has diminished it is essential that they practice active movements. For example, the subjects perform any specific task under the guidance of a physiotherapist or a caregiver. To provide such therapy with a robotic rehabilitation protocol, the robotic devices will guide the subject's movement to complete the specified task. Further studies reveal that enhanced motor learning occurs in the 'active rehabilitation therapy' mode, when patients (independently) practice a variety of functional tasks (Winstein, Merians et al. 1999) such as grasping and reaching movements and receive feedback (e.g., visual and haptic feedback) intermittently (Winstein, Miller et al. 2003, Lum, Burgar et al. 2004). However, no such robot has existed to provide such guided rehabilitation.

To contribute in this area, in this research we have proposed to develop a robot guided rehabilitation scheme for upper extremity rehabilitation. A humanoid robot, NAO was used for this purpose. NAO has 25 degrees of freedom. With its sensors and actuators, it can walk forward and backward, can sit down and stand up, can wave his hand, can speak to the audience, can feel

the touch sensation, and can recognize the person he is meeting. All these qualities have made NAO a perfect coach to guide the subjects to perform rehabilitation exercises.

1.1 Research Objectives

The *specific aims* of this research project are:

Aim-1: to develop a library of active rehabilitation exercises for NAO robot.

Aim-2: to develop a tele-rehabilitation scheme for NAO robot

Aim-3: to develop NAO guided supervised rehabilitation scheme

Experimental results reveal that NAO can be effectively used to supervise and guide the subjects in performing active rehabilitation exercises for shoulder and elbow joint movements. This thesis is organized as follows:

Chapter 2: Humanoid Robot, NAO

This chapter outlines the overall design and specifications of NAO. It gives the reader an overall sense of the complete hardware package and the components that comprise it.

Chapter 3: Motion Capture System Kinect and Kinematics

Chapter 3 describes Kinect sensor and human upper-extremity kinematics. The modified DH notations were used to develop the kinematic modeling.

Chapter 4: NAO's Rehabilitation Library (NRL)

This chapter describes NAO's graphical programming interface (Choregraphe). A library of rehabilitation exercises for NAO (NRL) was developed in Choregraphe environment.

Chapter 5: Tele-rehabilitation scheme

This chapter presents a tele-rehabilitation scheme. It is expected a therapist can remotely tele-operate the NAO in real-time to instruct and demonstrate the subjects different arm movement exercises. Kinect sensor was used in this scheme to get tele-operator's kinematics data.

Chapter 6: NAO guided supervised rehabilitation

This chapter presents experimental results of **NAO guided supervised rehabilitation.**

Chapter 7: Conclusions and Recommendations

Finally, the Conclusions section of the paper summarizes the research outcomes and suggests directions for further research in section Recommendations.

CHAPTER 2

HUMANOID ROBOT NAO

Humanoid robot NAO, developed by Aldebaran Robotics, is one of the most promising autonomous programmable robot (Robotics). According to the SoftBank Robotics, currently almost 9000 NAO's are in use throughout the world and showing success in the fields of research and education (Robotics). At the year, 2004 Aldebaran first reveals NAO, which was developed under 'Project NAO'. NAO has drawn the attention of all the people due to its capability of human like acrobatic movement and human like communication capability such as vision, speech, hearing and touch sensing capability. All these functionalities in NAO's were make possible due to its facilities with 25 joints' motions along with two cameras, four microphones, two loud speakers, nine tactile sensors, and eight pressure sensors (Robotics).With its 25 degree of freedoms it can mimic almost all-simple human motion. NAO can do all simple human motions such as walking forward and backward, sitting down and standing up, waving hand, playing soccer etc. However, its technical background is not as simple as it looks like. NAO has different types of sensors, actuators, onboard processors etc. Different version of NAO robots is available now. In this research we have used NAO V5. Technical details for this version is described in next section.

2.1 Technical Overview:

Technical details of NAO robot is provided in Aldebaran documentation(SoftbankRonotics,2013)

2.1.1 NAO's Structural Details:

NAO V5 is 574 mm tall and 275 mm width with 5.4 kg body weight. Its upper arm length is 105 mm and lower arm length is 55.95 mm. Its thigh length 100 mm, tibial length 102.90 mm and foot height 45.19 mm.

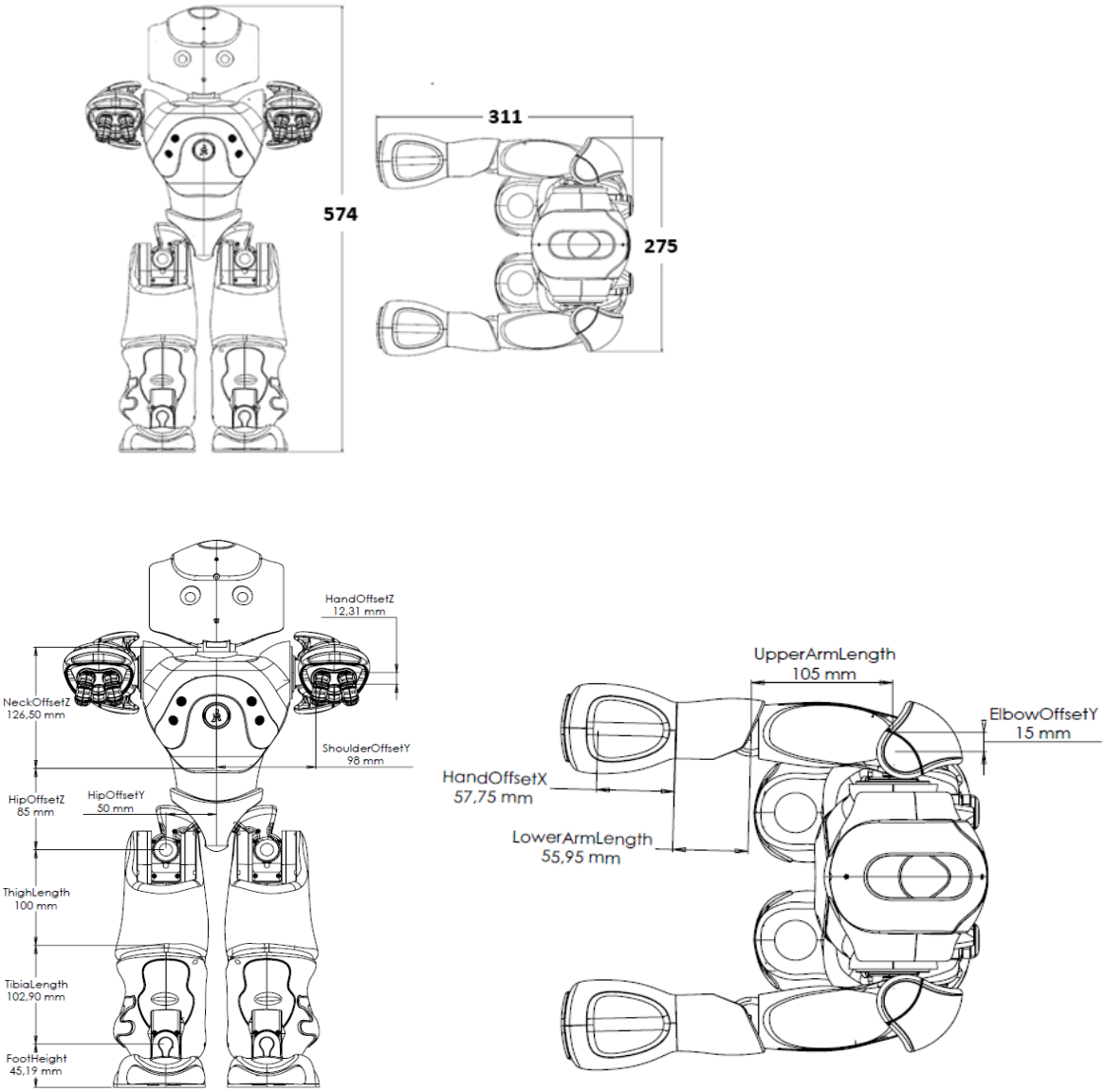

Figure 2.1 Dimensions of NAO robot

NAO has total 25 joints. Two joints in head, five joints in each arm along with hand close and open motions, five joints in each leg and two hip joints.

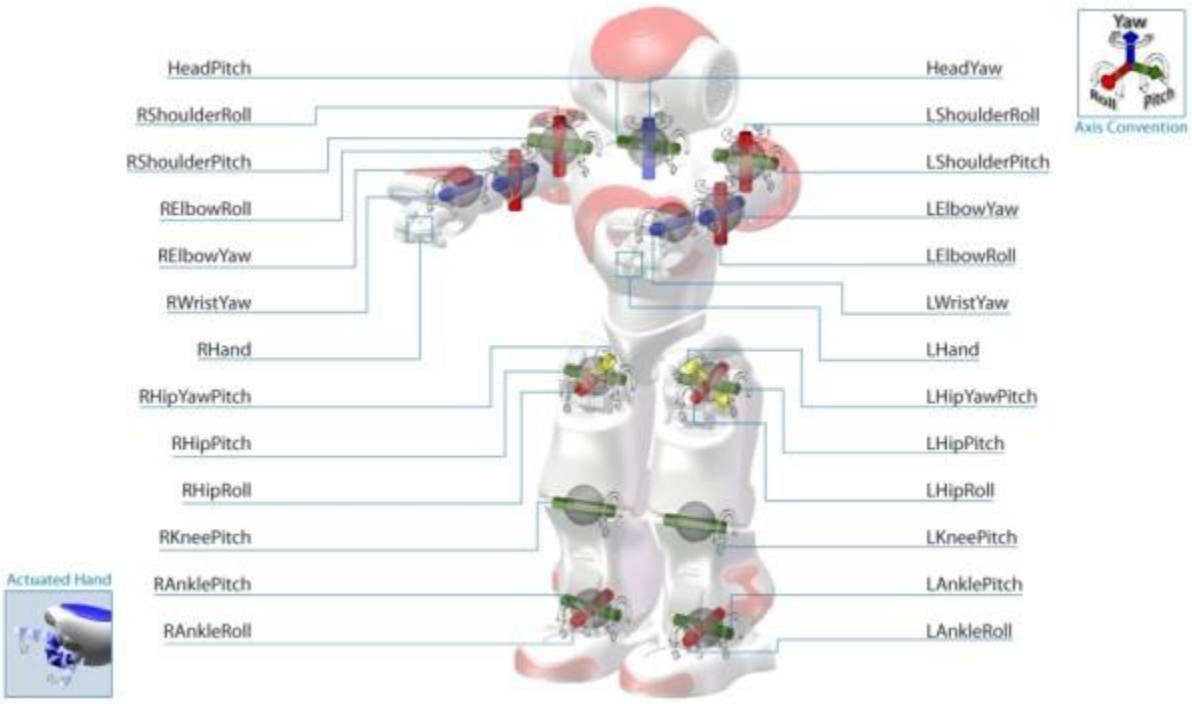

Figure 2.2 All joints in NAO robot (SoftbankRonotics,2013)

Axis convention and its joints' range of motion are shown in figure below. Note that NAO has 25DOF.

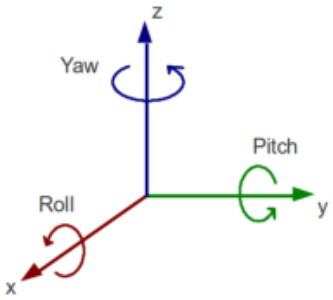

(a) Sign convention

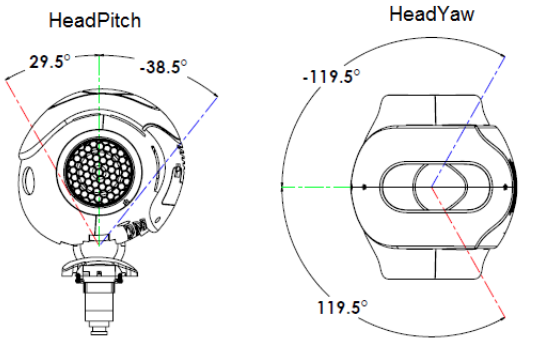

(b) Head pitch (Side view) and Head yaw (Top view)

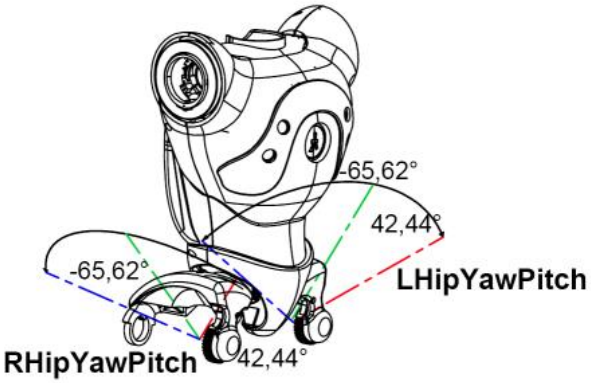

(c) Hip joint right yaw pitch and left yaw pitch

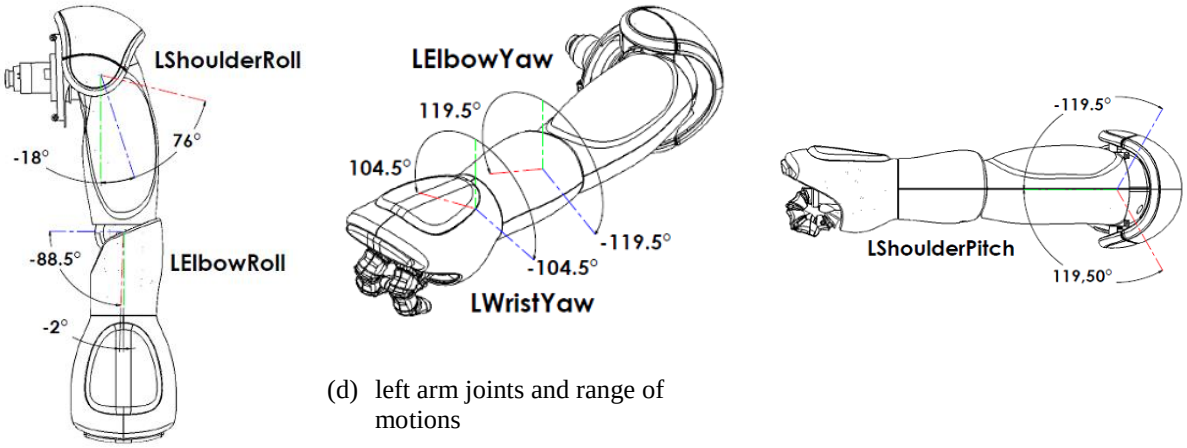

(d) left arm joints and range of motions

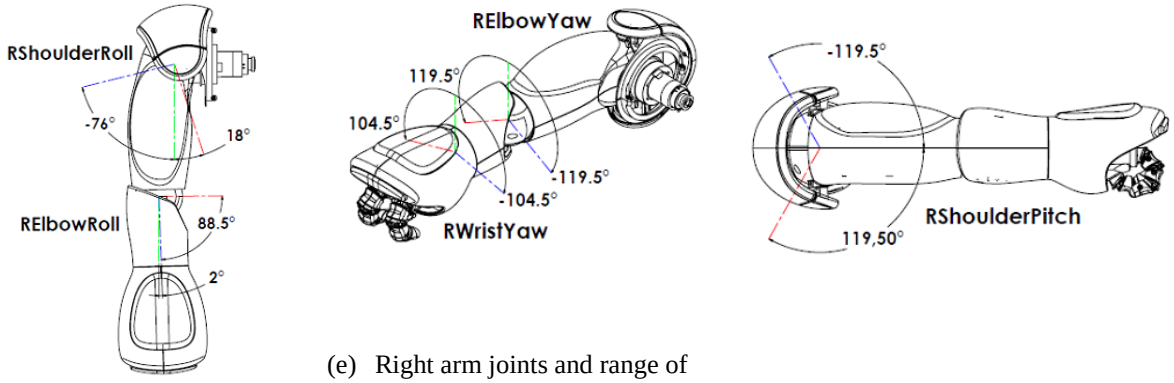

(e) Right arm joints and range of motions

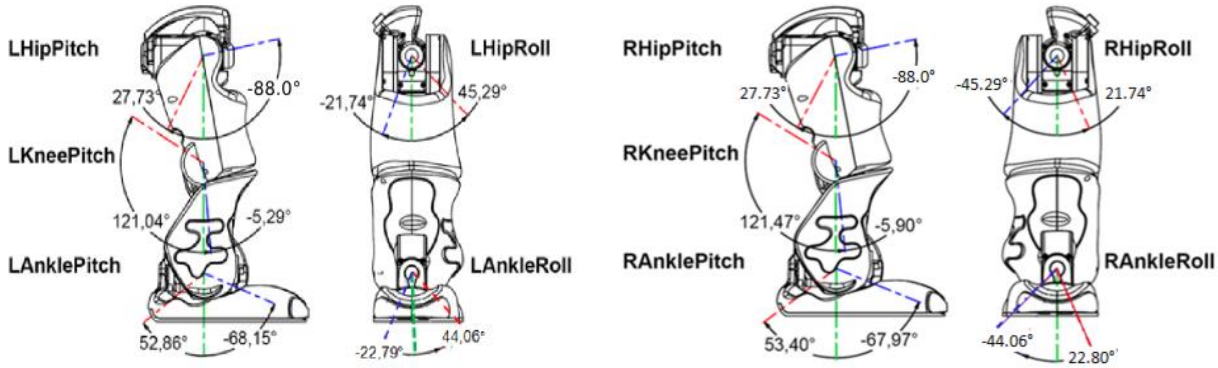

(f) Left leg joints and range of motion

(g) Right leg joints and range of motion

Figure 2.3 All joints of NAO robot with range of motion (SoftbankRonotics,2013)

In this study, we focused on upper extremity rehabilitation scheme, therefore, throughout the study we have focused on the upper arm (right) of the NAO. The range of motion of NAO is slightly different compared to human upper arm range of motion. For instance, its elbow joint range of motion is less compare to the human elbow joint motion. In addition, NAO's shoulder joint roll motion range is smaller compare to that of human shoulder joint motion. On the other

hand, its shoulder pitch range of motion is larger compare to the human shoulder joint pitch motion.

Human upper-extremity joints motions are depicted in Figure 2.4.

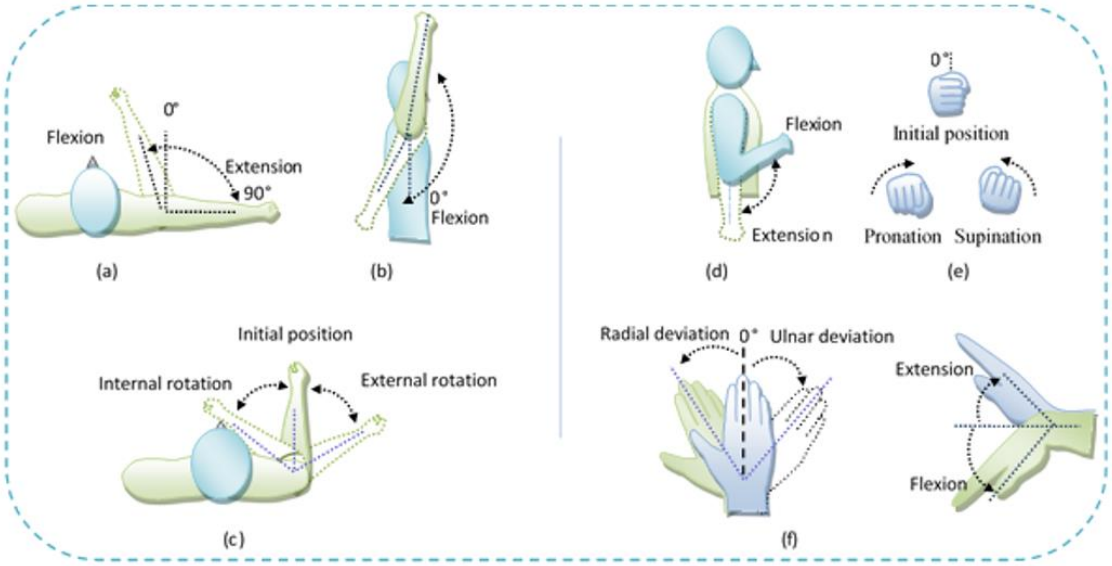

General motion. **(a)** Joint-1: shoulder joint horizontal flexion-extension; **(b)** Joint-2: shoulder joint vertical flexion-extension; **(c)** Joint-3: shoulder joint internal-external rotation; **(d)** Joint-4: elbow flexion-extension; **(e)** Joint-5: forearm pronation-supination; **(f)** Joint-6: wrist joint radial-ulnar deviation; **(g)** Joint-7: wrist joint flexion-extension.

Figure 2.4 Upper-extremity joints motion

Table 2.1 summarizes upper extremity range of motion of NAO robot.

Table 2.1 Joint motion range of NAO and human arm

Joint Name	Motion	Range for NAO	Range for human
RshoulderPitch	Right shoulder joint front and back (Y)	-119.5 to 119.5	-150 to +30
RshoulderRoll	Right shoulder joint right and left (Z)	-76 to 18	−50 to +180
RElbowRoll	Right elbow joint (Z)	2 to 88.5	0 to +150
RElbowYaw	Right shoulder joint twist (X)	-119.5 to 119.5	−90 to +15

2.1.2 NAO's Motherboard:

NAO has its own central processing unit (CPU) to execute command and control all the sensors. Its motherboard consists of Intel ATOM 2530 1.6 GHz processor with cache memory 512KB, clock speed 1.6 GHZ and FSB speed 533mHz, 1GB RAM, 2GB flash memory and 8GB Micro SDHC. In addition, it provides communication through WiFi using IEEE 802.11 a/b/g/n protocol, Ethernet, and USB interface. Its USB port mainly used for updating the robot operating system.

2.1.3 NAO's Sensors, Vision and Audio System

To explore the surroundings, to take a command from the user, and to give feedback information both to the control unit and to the user, NAO is equipped with different types of sensors, vision and audio system.

2.1.3.1 Vision

Two identical video cameras which are located in the forehead of NAO provide its vision system. Each camera is a kind of SOC image sensor with 1.22 MP resolution and optical format 1/6 inch active pixels (HxV) 1288x968, dynamic range 70 dB. Field of view 72.6ºDFOV

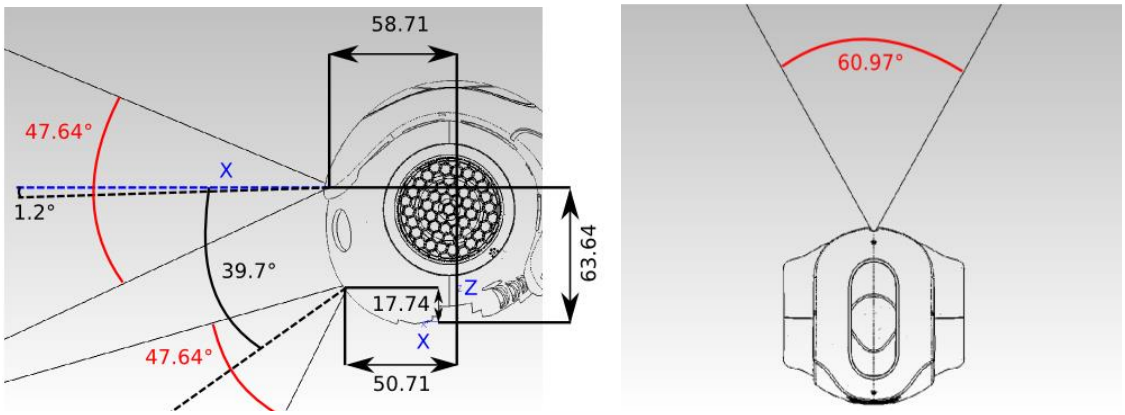

Figure 2.5 NAO's Camera (SoftbankRonotics,2013)

(60.9ºHFOV, 47.6ºVFOV). Focus range 30cm to infinity. Camera data streaming rate 30fps. Through this vision system, NAO can detect human face, object, provide live video streaming for image processing etc.

2.1.3.2 Audio:

NAO provides a stereo broadcast system made up of two loudspeakers in its ears and four microphones on its head to detect sound.

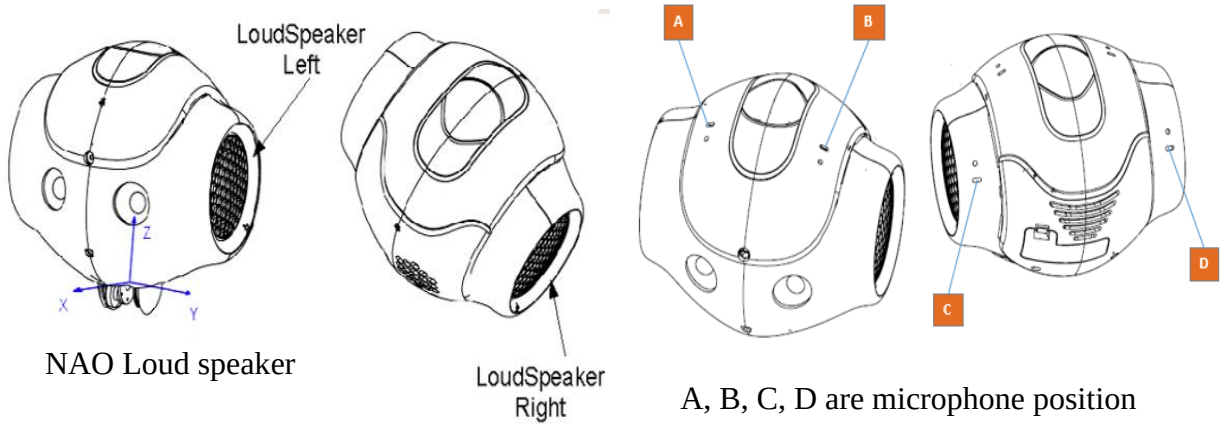

Figure 2.6 NAO audio system (SoftbankRonotics,2013)

2.1.3.3 Sensors:

NAO is equipped with different contact sensors that are used to sense touch on this particular area. There are three tactile sensors on its head to sense any touch on its head. Three tactile sensor on each hands and two feet bumpers located at the tip of each foot, which are mainly used to detect obstacles. NAO also has four force sensitive resistors (FSR) in each foot with range of 0 N to 25N. These sensors are used to measure applied pressure on foot that help it to walk.

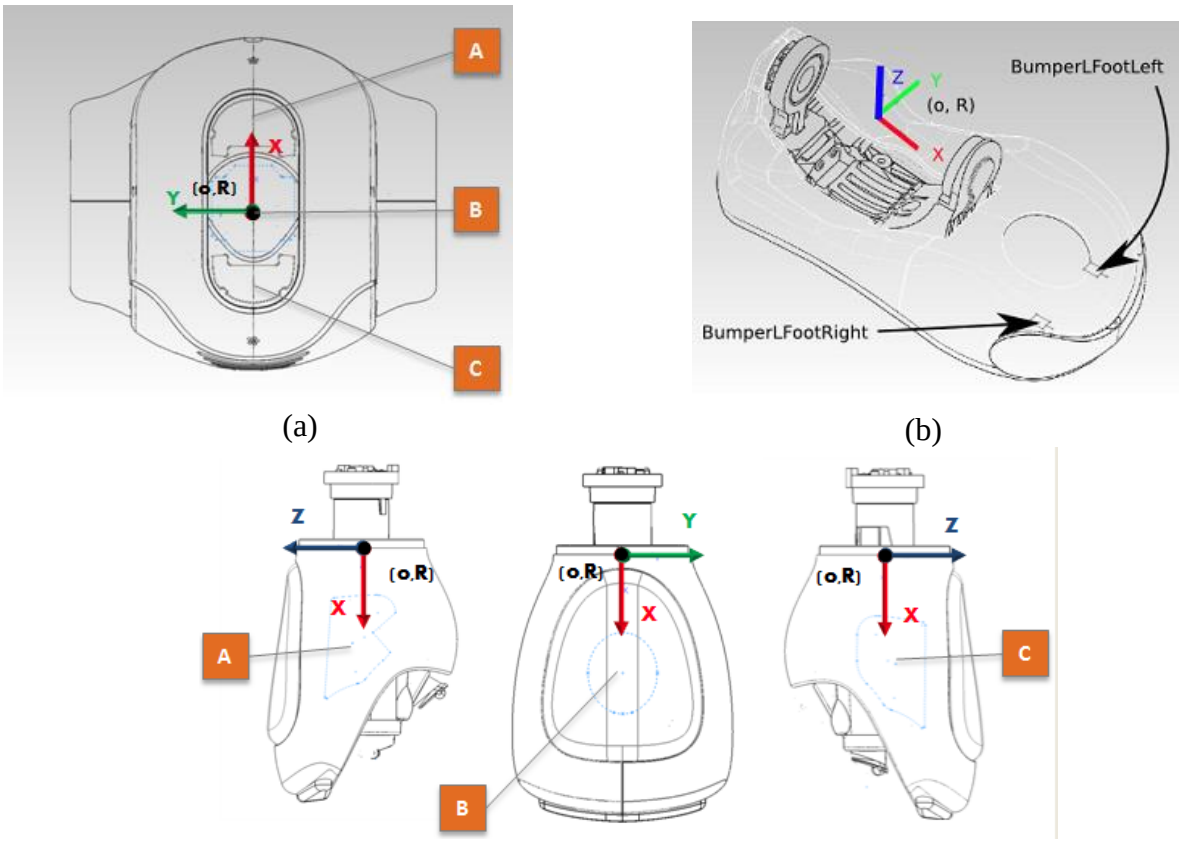

(a) tactile sensor position in head, (b) foot bumper position, (c) tactile sensor position in hand

Figure 2.7 NAO's tactile sensor and bumper sensor locations(SoftbankRonotics,2013)

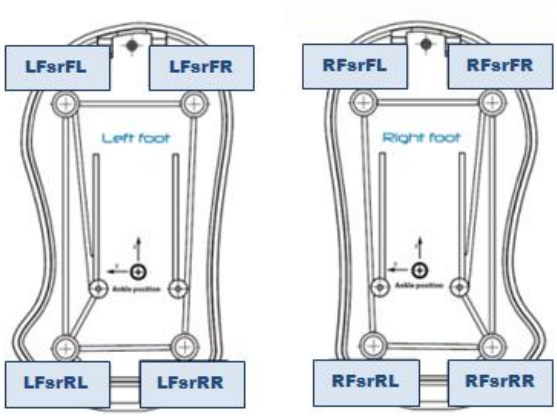

Figure 2.8 Force sensitive resistors(FSR) location on the feet of NAO (SoftbankRonotics,2013)

To detect obstacles and measure the distance between the obstacles and NAO there are two sonar emitters and two sonar receivers located at NAO's chest with range of 0.20 m to 0.80 m. Under 20cm no distance information can be provided. Effective cone for the sensors is 60º.

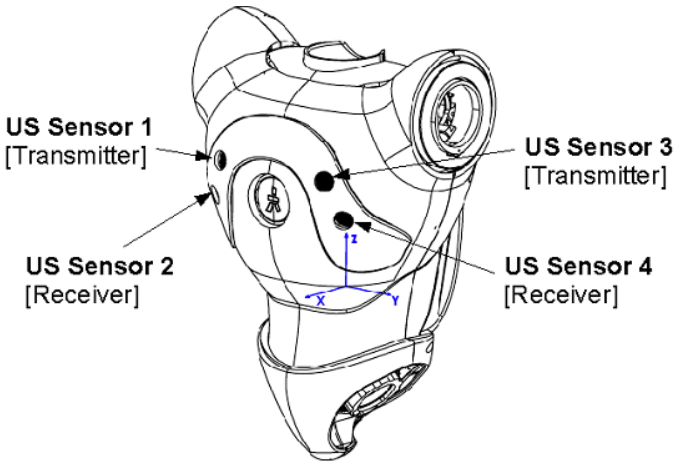

Figure 2.9 Sonar sensor location(SoftbankRonotics,2013)

NAO has two IR sensors on its face which are used to communicate with other NAO robot, take command from IR remote etc. For balance control and orientation control NAO is equipped with inertial unit located inside the torso. Inertial unit consists of one 3-axis gyrometer and one 3-axis accelerometer. To determine the joint position NAO's motors are equipped with magnetic rotary encoder (MRE) (precision of 0.1º).

2.2 NAO's Operating System

NAOqi is an embedded software, which always runs on NAO's operating system, NAOqi OS. To control the robot one need to communicate with this software. To facilitate communication

with NAOqi we need to use NAOqi Software Development Kit (SDK). NAOqi SDK is actually a set of application programming interfaces (API) which vary for different programming platform. The Softbank robotics provides API for C++, Python and Java to develop application for NAO.

NAOqi OS is the main operating system for NAO robot, which is a GNU/Linux distribution based on Gentoo. It provides all necessary libraries and programs that are required to operate NAOqi. NAOqi OS compatible with other operating system such as Windows, Mac, Linux. In the NAOqi OS the main programming framework that is used to program NAO is NAOqi framework (2013). Homogeneous communication between different modules (motion, audio, video), homogeneous programming, and homogeneous information sharing all are possible through this framework. This framework provides a cross-platform, cross language and introspection support. Introspection means this framework knows which functions are available in the different modules and where. Parallelism, resources, event management, synchronization all basic robotics need fulfilled by this framework.

NAOqi software in NAOqi OS is actually a broker that defines which libraries it should be loading. Different methods which control the robot functionality are contained in modules where one or more module contained in a library. So methods are attached to modules and modules are attached to a broker. So, mainly broker provides directory and network access service through the proxy where a proxy is an object that represents to which module broker need to call. A programmer can call any methods in the module by using a proxy object for a particular module where the proxy modules are provided in the API.

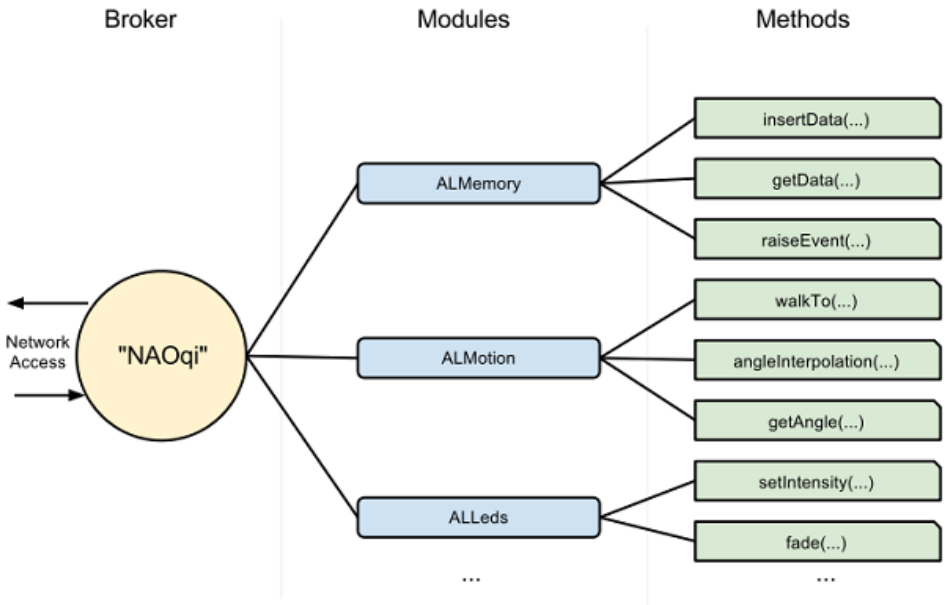

Figure 2.10 NAOqi work process

2.3 NAO Programming:

We can build behavior for NAO by using a high level block based programming environment called Choregraphe (Sahrmann and Norton 1977) or by using other programming languages for which appropriate API is available. Choregraphe is a multi-platform desktop application that can create complex behaviors without writing any code. It is actually a graphical programming interface. Different functionalities of NAO are represented here as behavior blocks. All those blocks provide specific task for NAO. By combining different blocks, one can create new behavior block. Like LabVIEW and Simulink, Choregraphe use same concept of signal flow and executes the blocks in order they are connected to each other. It provides lots of built in behavior blocks that can perform specific task. The build behavior in Choregraphe can be tested in a virtual NAO or it can be implemented as a permanent behavior in physical NAO. In addition, Choregraphe

provides behavior control of NAO. One can remove an old behavior or can add a new behavior through this. It is very user friendly. Options are available to create new behavior blocks for advanced functionality (of NAO) in Choregraphe by using programming language python with python API.

For code programming Aldebaran provides API for language C++, Python and Java for NAO V5. Python SDK for NAO robot requires Python 2.7-32 bits. It only works for this environment (Python 2.7-32 bits). C++ SDK requires a C++ compiler for different OS. For Windows, C++ SDK only works for Visual Studio 2010. Windows also have some limitations, there is no C++ cross compiler. As a solution to this problem, Windows users need to install qiBuild, a tool design to generate cross platform projects using CMake along with the C++ SDK. In our study, we have used Python 2.7.13 and Python SDK to control the NAO for advanced functionality.

CHAPTER 3

KINECT MOTION CAPTURE SYSTEM AND KINEMATICS

To analyze human upper extremity kinematics, it is necessary to capture the upper arm motion. Now a day's various types of motion capture devices are available. In this research, we have used Kinect V2 sensor (Microsoft 2017) for this purpose. Kinect sensor provided by Microsoft, has a depth sensor, a color camera, and a four microphone array. It can track full body of a person. Due to its low price cost Kinect is used for different applications in different fields.

Figure 3.1 Kinect sensor(Microsoft 2017)

3.1 Technical details

Microsoft Kinect is equipped with a IR depth sensor, one RGB camera and a four microphone array. Using depth sensor it can produce a 3D depth image with regulation 512x424 at 30 FPS (frame per sec) and range 0.5 to 8 meters. It provides light independent infrared and able to remove ambient light effect. RGB camera provide full HD 1920 x 1080 regulation. Provide either 30 or 15 FPS based on lighting. Most amazing feature of Kinect sensor is that it can track a full human body. It can track 25 joints in human body with clear identification of hand states whether it is

open or close. Body joint tracking means it provide the coordinates of each joint in 3D space. It can track a total of six-persons simultaneously in front of it within a range of 0.5 to 4.5 meters. Through the microphone, it also can detect sound direction. Field of view of its depth camera is 70º in horizontal and 60º in vertical direction.

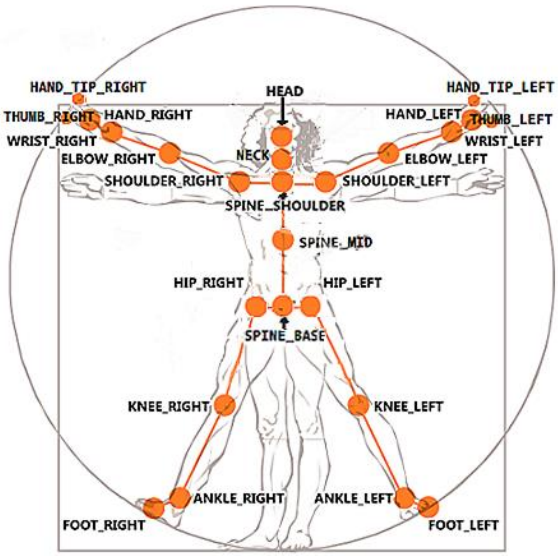

Figure 3.2 Name of the tracked joints using Kinect (Microsoft 2017)

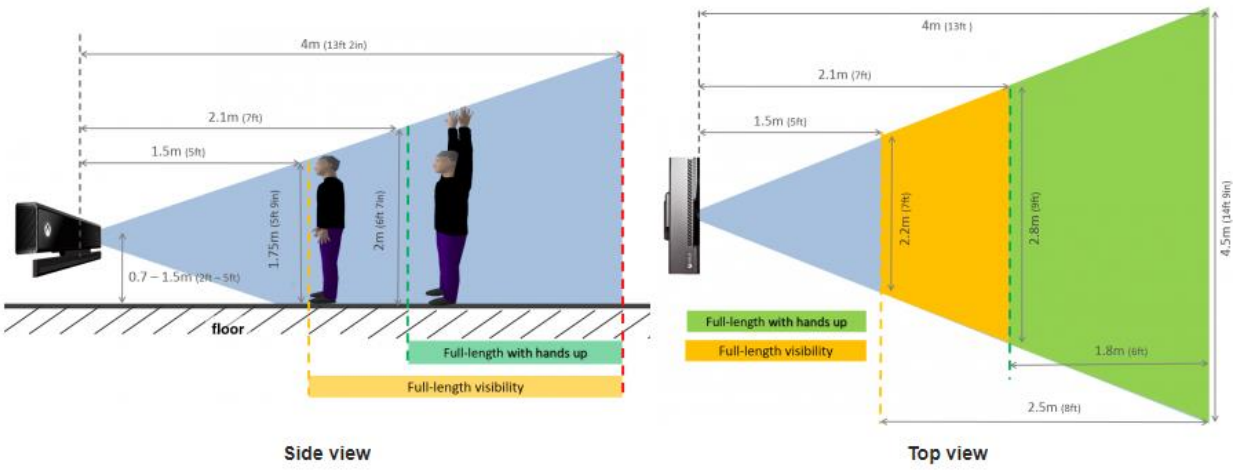

Figure 3.3 Field of view of Kinect sensor(Wiki)

Kinect V2 came with the software development kit (SDK) by which one can extract Kinect data through programming. Kinect V2 SDK is compatible only with the Microsoft Visual Studio 2012 or its higher version. To run this SDK the windows operating system must be windows 8 or higher with 64-bit processor and minimum 4 GB memory. Data can be streamed only through the USB 3.0 port.

3.2 Data extraction from Kinect

To access the Kinect data we used Kinect V2 SDK. This SDK provides necessary API to extract Kinect data using Visual studio 2012 or higher. It is (SDK) compatible with programing language C++, C#, Java.

In this research, we have extracted Kinect data to analyze human arm kinematics and also to tele-operate the NAO (in real-time) to establish the proposed tele-rehabilitation scheme.

As mentioned in Chapter-3 to control the NAO robot, C++ language can be used with proper SDK. If C++ is used for both NAO and Kinect then this two systems can be operated in a same platform. However, the SDK provided for this NAO robot is only compatible with Visual studio 2010, and Kinect V2 SDK only works with Visual studio 2012 or its higher version. That is why, it is difficult to control two systems in a common platform. Therefore, for NAO robot we use Python 2.7 32bit. In addition, data analysis in C++ need too much coding and debugging of C++ code is little bit difficult. As, C++ is a low level programming language, it may cause serious trouble to the processor due to bugs in the coding. For all these reasons, we used MATLAB to extract data from Kinect. Microsoft does not provide any SDK for MATLAB. But there is a toolbox call Kin2 (Terven and Córdova-Esparza 2016) developed in MATLAB to extract data from Kinect. We used

this toolbox for our study. This toolbox actually call C++ function from MATLAB by using MAX function. Main data extraction code is written in C++. To use this toolbox a C++ compiler is required. In our case, we used Visual studio 2015. However, the performance of the Kin2 application is not as fast as a native C++ application (Terven and Córdova-Esparza 2016). Through this toolbox, we access color, depth and body index frames in real time. The color frame contains the information of pixel value along with the position information in 2D plane. Where depth frame contains the information of the pixel in 2D plane along with the depth information of each pixel. From this depth data, Kinect provides the coordinate information of the tracked position on the image. As mentioned earlier Kinect can track 25 joints in the human body. However, in this study, our focus was on human upper extremity. To serve our purpose, we tracked only 11 joints in human upper extremities that includes shoulder, elbow and wrist joint in each arm along with the head, neck, spine shoulder, spine mid and spine base joint. We eliminated other joint tracking and the infrared tracking from main C++ code as well as from the Kin 2 program to increase the performance.

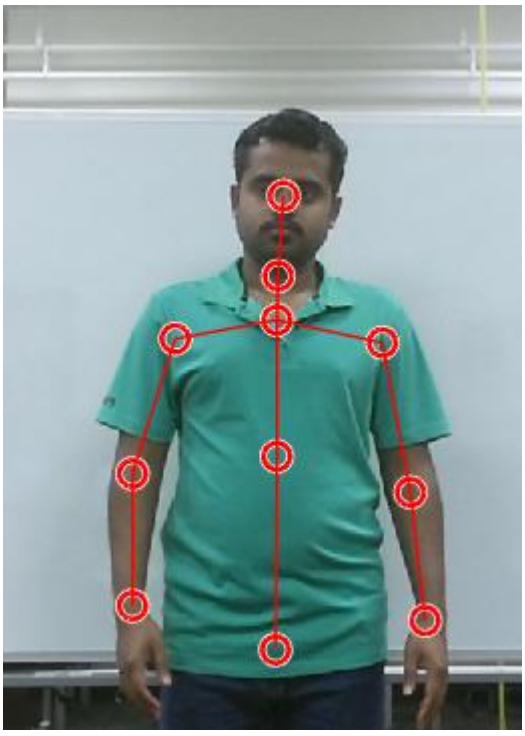

Figure 3.4 Tracked 11 joints in human body upper extremities

3.3 Joint parameter from Kinect data

From the Kinect data we obtained the joint coordinates of each joint. For the purpose of our study we focus on human right arm's kinematics. To model the kinematics of human arm modified DH conventions were used(Craig 2005). For this purpose, every joints are assigned with a coordinate frame. The coordinate frame assignment and DH parameters determination procedures are described in following section.

3.3.1 Coordinate frame assignment

There are different ways to assign coordinate frames to each joint to determine the kinematic. For our study we have followed the modified Denavit-Hartenberg method. (Denavit and Hartenberg 1955, Craig 2005). The steps of coordinate frame assignment are given below (Hartenberg and Denavit, 1964:

- assume each joint motion is generated from one DoF revolute joint
- determine the axes of rotation and denote each axis as $Z_0, \ldots\ldots, Z_n$;
- locate the origin of each link-frame (O_i) where the common perpendicular line between the successive joint axes (i.e., Z_{i-1} and Z_i) intersects. If the joint axes are not parallel, locate the link-frame origin at the point of intersection between the axes;
- locate the X_i axis (at link frame origin O_i) as pointing along the common normal line between the axes Z_{i-1} and Z_i. If the joint axes intersect, establish X_i in a direction normal to the plane containing both axes (Z_{i-1} and Z_i);
- establish the Y_i axis through the origin O_i to complete a right-hand coordinate system.

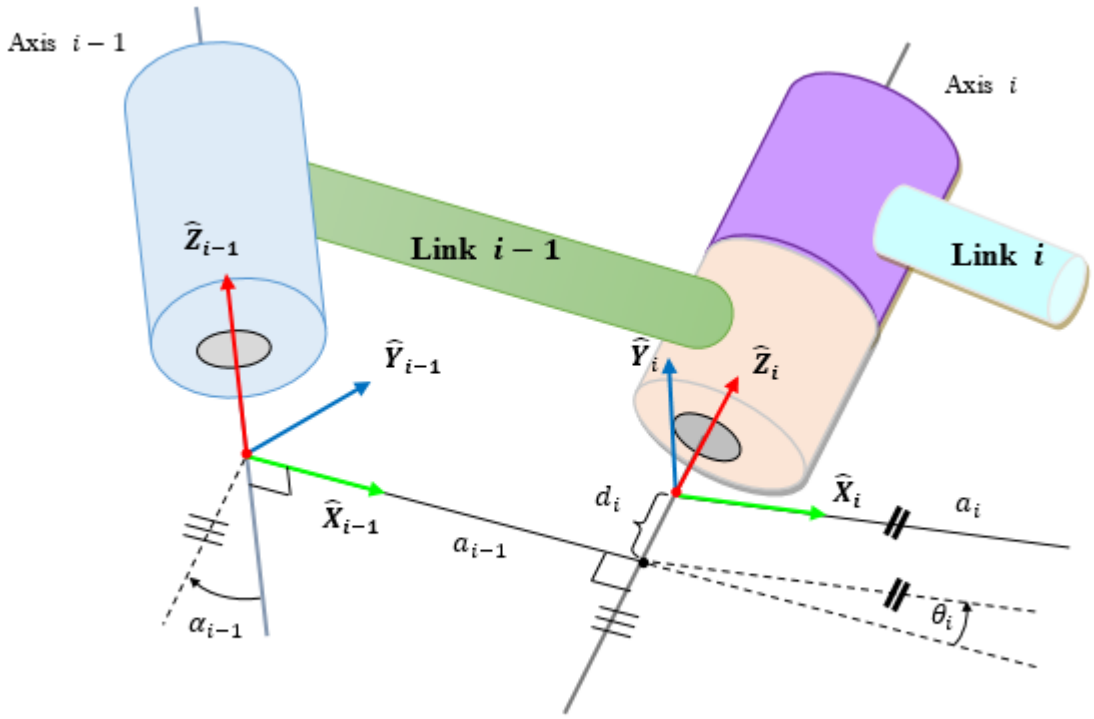

Figure 3.5 Coordinate frame assignment Adaoted from Craig

3.3.2 D-H parameters

A link of a robot can be described by four parameters (two parameters for describing the link itself and other two for describing the link's relation to a neighboring link) if we assign the co-ordinate frames as described above (Denavit and Hartenberg, 1955). These parameters are known as Denavit-Hartenberg (DH) parameters. The definitions of the DH parameters are given below (Hartenberg and Denavit, 1964):

Link Length (ai) : the length measured along Xi, from axis Zi to axis Zi+1;

Link Twist (αi) : the angle measured about Xi, from axis Zi to axis Zi+1;

Link Offset (di) : the distance measured along the axis Zi; from Xi-1 to Xi, and

Joint Angle (θi) : the angle measured about Zi, from Xi-1 to Xi

To obtain the DH parameters, we assume that the co-ordinate frames (i.e., the link-frames which map between the successive axes of rotation) coincide with the joint axes of rotation and have the same order, i.e., frame coincides with joint 1, frame {2} with joint 2, and so on.

As shown in Figure 3.2, the joint axes of rotation of the human right upper limb are indicated by dark black arrow heads (i.e., Zi). In this model, joints 1, and 2 together constitute the shoulder joint, where joint 1 corresponds to abduction/adduction joint 2 represents vertical flexion/extension, joint 3 corresponds to internal/external rotation of the shoulder joint and joint 4 represents the flexion/extension of the elbow joint. The elbow joint is located at a distance d_{upper_arm} and wrist joint is located at a distance $d_{forearm}$. The modified DH parameters corresponding to the placement of the link frames (in Figure 3.5) are summarized in Table 4.1.

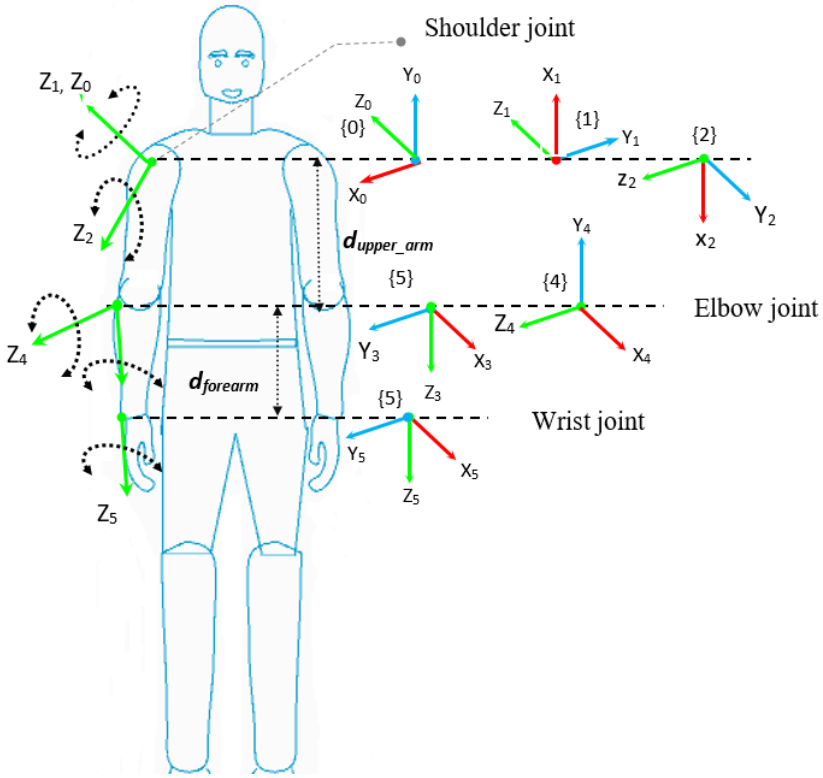

Figure 3.6 Link frame attachments to the human right limb

These DH parameters are used to get the homogeneous transfer matrix, which represents the positions and orientations of the reference frame with respect to the fixed reference frame. It is assumed that the fixed reference frame {0} is located at the same point of the first reference frame {1}.

Table 3.1 Modified Denavit-Hartenberg parameters

Joint *(i)*	α_{i-1}	d_i	a_{i-1}	θ_i
1	0	*0*	0	θ_1- π/2
2	π/2	0	0	θ_2
3	π/2	d_{upper_arm}	0	θ_3
4	-π/2	0	0	θ_4
5	π/2	$d_{forearm}$	0	*0*

where, α_{i-1} is the link twist, a_{i-1} corresponds to link length, d_i stands for link offset, and θ_i is the joint angle of human arm.

We know that the general form of a link transformation that relates frame $\{i\}$ relative to the frame $\{i-1\}$ (Craig 2005) is:

$$ {}^{i-1}_{i}T = \begin{bmatrix} {}^{i-1}_{i}R^{3\times3} & {}^{i-1}_{i}P^{3\times1} \\ 0^{1\times3} & 1 \end{bmatrix} \tag{3.1} $$

where, ${}^{i-1}_{i}R$ is the rotation matrix that describes frame $\{i\}$ relative to frame $\{i-1\}$ and can be expressed as:

$$ {}^{i-1}_{i}R = \begin{bmatrix} \cos\theta_i & -\sin\theta_i & 0 \\ \sin\theta_i \cos\alpha_{i-1} & \cos\theta_i \cos\alpha_{i-1} & -\sin\alpha_{i-1} \\ \sin\theta_i \sin\alpha_{i-1} & \cos\theta_i \sin\alpha_{i-1} & \cos\alpha_{i-1} \end{bmatrix} \tag{3.2} $$

and, ${}^{i-1}_{i}P$ is the vector that locates the origin of frame $\{i\}$ relative to frame $\{i-1\}$ and can be expressed as:

$$ {}^{i-1}_{i}P = [a_{i-1} \quad -s\,\alpha_{i-1}\,d_i \quad c\,\alpha_{i-1}\,d_i]^T \tag{3.3} $$

Using Equations (3.1) to (3.3) the individual homogeneous transfer matrix that relates two successive frame (of figure) can be found as:

$$
{}^{0}_{1}T = \begin{bmatrix} \cos\left(\theta_1 + \frac{\pi}{2}\right) & -\sin\left(\theta_1 + \frac{\pi}{2}\right) & 0 & 0 \\ \sin\left(\theta_1 + \frac{\pi}{2}\right) + & \cos\left(\theta_1 + \frac{\pi}{2}\right) & 0 & 0 \\ 0 & 0 & 1 & 0 \\ 0 & 0 & 0 & 1 \end{bmatrix},
$$

$$
{}^{1}_{2}T = \begin{bmatrix} \cos\left(\theta_2 - \frac{\pi}{2}\right) & -\sin\left(\theta_2 - \frac{\pi}{2}\right) & 0 & 0 \\ 0 & 0 & -1 & 0 \\ \sin\left(\theta_2 - \frac{\pi}{2}\right) & \cos\left(\theta_2 - \frac{\pi}{2}\right) & 0 & 0 \\ 0 & 0 & 0 & 1 \end{bmatrix}
$$

$$
{}^{2}_{3}T = \begin{bmatrix} \cos\theta_3 & -\sin\theta_3 & 0 & 0 \\ 0 & 0 & -1 & -d_{upper\_arm} \\ \sin\theta_3 & \cos\theta_3 & 0 & 0 \\ 0 & 0 & 0 & 1 \end{bmatrix},
$$

$$
{}^{3}_{4}T = \begin{bmatrix} \cos\theta_4 & -\sin\theta_4 & 0 & 0 \\ 0 & 0 & 1 & 0 \\ -\sin\theta_4 & -\cos\theta_4 & 0 & 0 \\ 0 & 0 & 0 & 1 \end{bmatrix}
$$

$$
{}^{4}_{5}T = \begin{bmatrix} cos\,\theta_5 & -sin\,\theta_5 & 0 & 0 \\ 0 & 0 & -1 & -d_{forearm} \\ sin\,\theta_5 & cos\,\theta_5 & 0 & 0 \\ 0 & 0 & 0 & 1 \end{bmatrix}
$$

The homogenous transformation matrix that relates frame {7} to frame {0} can be obtained by multiplying individual transformation matrices.

$$
{}^{0}_{5}T = [{}^{0}_{1}T.\,{}^{1}_{2}T\,{}^{2}_{3}T.\,{}^{3}_{4}T.\,{}^{4}_{5}T] \qquad (3.4)
$$

The single transformation matrix thus found from Equation (3.4) represents the positions and orientations of the reference frame attached to the wrist joint (axis 5) with respect to the fixed reference frame {0}. The equation obtained from this transformation matrix is known as forward

kinematics equation. If the joint variable of each joint ($\theta_1, \theta_2, \theta_3$ and θ_4) is given then from this forward kinematics equation the position of list frame can be determined.

3.3.3 Inverse Kinematics

Analytical approach:

In our case we already got the joint coordinate for shoulder joint (x_{sk}, y_{sk}, z_{sk}), elbow joint(x_{ek}, y_{ek}, z_{ek}) and wrist joint (x_{wk}, y_{wk}, z_{wk}) form Kinect with respect to Kinect coordinate frame (as shown in Figure 3.1). We needed to determine the angle of rotation for each joint ($\theta_1, \theta_2, \theta_3$ and θ_4) from Kinect data which is inverse kinematics problem. However, the problem is to find a closed form solution due to nonlinear nature of the equation; sometimes multiple solutions may also exist. To solve the inverse kinematics first we need two-transformation matrix ${}^0_3T$and ${}^0_5T$ to represents the positions and orientations of the frame attached to the elbow joint (axis 3) and the wrist joint (axis 5) with respect to the fixed reference frame {0} and also we transfer the coordinate from Kinect coordinate frame to frame { 0}. The orientation of frame {0} is identical to Kinect coordinate frame, So, we got the coordinate of elbow (frame (Mozaffarian, Benjamin et al.) and {4}) and wrist (frame {5}) joint with respect to frame {0} by subtracting shoulder joint coordinate from elbow and wrist joint coordinate which is obtained from Kinect. Then the new shoulder joint coordinate (x_s, y_s, z_s) equal to (0,0,0) and elbow joint coordinate (x_e, y_e, z_e) equal to ($x_{ek} - x_{sk}, y_{ek} - y_{sk}, z_{ek} - z_{sk}$) and wrist joint coordinate (x_w, y_w, z_w) equal to ($x_{wk} - x_{sk}, y_{wk} - y_{sk}, z_{wk} - z_{sk}$). Now.

$$ {}^0_3T = [{}^0_1T.\,{}^1_2T\,{}^2_3T] = \begin{bmatrix} r11 & r12 & r13 & P_x \\ r21 & r22 & r23 & P_y \\ r31 & r32 & r33 & P_z \\ 0 & 0 & 0 & 1 \end{bmatrix} $$

Where, $P_x = d_{upper_{arm}} \cos(\theta_1 + {}^{\pi}/_{2}) \sin(\theta_2 - {}^{\pi}/_{2})$ (3.6)

$P_y = d_{upper_{arm}} \sin(\theta_1 + {}^{\pi}/_{2}) \sin(\theta_2 - {}^{\pi}/_{2})$ (3.7)

$P_z = -d_{upper_{arm}} \cos(\theta_2 - {}^{\pi}/_{2})$ (3.8)

Here, (P_x, P_y, P_z) represents the elbow joint coordinate (x_e, y_e, z_e).

$x_e = d_{upper\_arm} \cos(\theta_1 + {}^{\pi}/_{2}) \sin(\theta_2 - {}^{\pi}/_{2})$ (3.9)

$y_e = d_{upper\_arm} \sin(\theta_1 + {}^{\pi}/_{2}) \sin(\theta_2 - {}^{\pi}/_{2})$ (3.10)

$z_e = -d_{upper\_arm} \cos(\theta_2 - {}^{\pi}/_{2})$ (3.11)

Again, from

$$ {}^{0}_{5}T = [{}^{0}_{1}T . {}^{1}_{2}T {}^{2}_{3}T . {}^{3}_{4}T . {}^{4}_{5}T] = \begin{bmatrix} r11 & r12 & r13 & P_x \\ r21 & r22 & r23 & P_y \\ r31 & r32 & r33 & P_z \\ 0 & 0 & 0 & 1 \end{bmatrix} $$

Where,

$$ P_x = d_{forearm}(\sin\theta_4 \sin\theta_3 \sin(\theta_1 + {}^{\pi}/_{2}) + \cos\theta_3 \cos(\theta_1 + {}^{\pi}/_{2}) \cos(\theta_2 - {}^{\pi}/_{2}) + \cos\theta_4 \cos(\theta_1 + {}^{\pi}/_{2}) \sin(\theta_2 - {}^{\pi}/_{2})) - d_{upper\_arm} \cos(\theta_1 + {}^{\pi}/_{2}) \sin(\theta_2 - {}^{\pi}/_{2}) \quad (3.12) $$

$$ P_y = d_{upper\_arm} \sin(\theta_1 + {}^{\pi}/_{2}) \sin(\theta_2 - {}^{\pi}/_{2}) - d_{forearm}(\sin\theta_4 \cos(\theta_1 + {}^{\pi}/_{2}) \sin\theta_3 - \cos\theta_3 \cos(\theta_2 - {}^{\pi}/_{2}) \sin(\theta_1 + {}^{\pi}/_{2}) - \cos\theta_4 \sin(\theta_1 + {}^{\pi}/_{2}) \sin(\theta_2 - {}^{\pi}/_{2})) \quad (3.13) $$

$$P_z = -d_{forearm}\left(\cos\theta_4 \cos\left(\theta_2 - {}^{\pi}/_{2}\right) - \cos\theta_3 \sin\theta_4 \sin\left(\theta_2 - {}^{\pi}/_{2}\right)\right) - d_{upper\_arm} \cos\left(\theta_2 - {}^{\pi}/_{2}\right) \quad (3.14)$$

Here, (P_x, P_y, P_z) represents the elbow joint coordinate (x_w, y_w, z_w).

$$x_w = d_{forearm}\left(\sin\theta_4 \sin\theta_3 \sin\left(\theta_1 + {}^{\pi}/_{2}\right) + \cos\theta_3 \cos\left(\theta_1 + {}^{\pi}/_{2}\right) \cos\left(\theta_2 - {}^{\pi}/_{2}\right) + \cos\theta_4 \cos\left(\theta_1 + {}^{\pi}/_{2}\right) \sin\left(\theta_2 - {}^{\pi}/_{2}\right)\right) - d_{upper\_arm} \cos\left(\theta_1 + {}^{\pi}/_{2}\right) \sin\left(\theta_2 - {}^{\pi}/_{2}\right) \quad (3.15)$$

$$y_w = d_{upper\_arm} \sin\left(\theta_1 + {}^{\pi}/_{2}\right) \sin\left(\theta_2 - {}^{\pi}/_{2}\right) - d_{forearm}\left(\sin\theta_4 \cos\left(\theta_1 + {}^{\pi}/_{2}\right) \sin\theta_3 - \cos\theta_3 \cos\left(\theta_2 - {}^{\pi}/_{2}\right) \sin\left(\theta_1 + {}^{\pi}/_{2}\right) - \cos\theta_4 \sin\left(\theta_1 + {}^{\pi}/_{2}\right) \sin\left(\theta_2 - {}^{\pi}/_{2}\right)\right) \quad (3.16)$$

$$z_w = -d_{forearm}\left(\cos\theta_4 \cos\left(\theta_2 - {}^{\pi}/_{2}\right) - \cos\theta_3 \sin\theta_4 \sin\left(\theta_2 - {}^{\pi}/_{2}\right)\right) - d_{upper\_arm} \cos\left(\theta_2 - {}^{\pi}/_{2}\right) \quad (3.17)$$

Equation (3.9), (3.10), (3.11), (3.15), (3.16) and (3.17) are our inverse kinematic analytical equation. There is four unknown but we have six equation, which are highly nonlinear and difficult to solve. To simplify the calculation we determine the joint angle θ_4 geometrically using cosine rule.

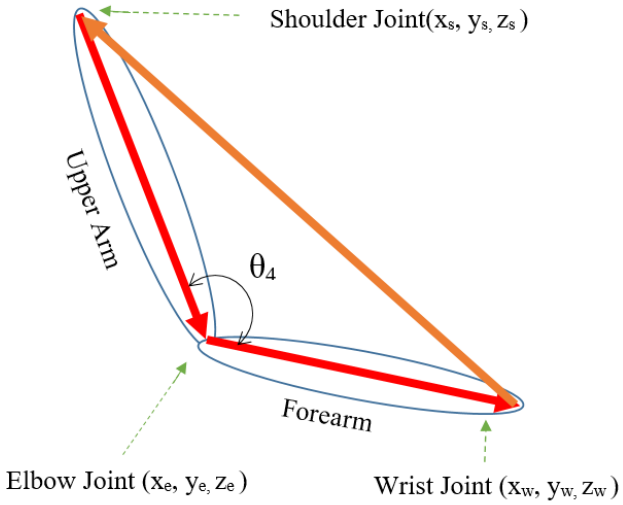

Figure 4.7 joint angle $\theta_4$calculation

Now, by the cosine rule

$$d^2 = d_{upper\_arm}^2 + d_{forearm}^2 - 2d_{upper\_arm}\, d_{forearm} \cos\theta_4$$

Then, $\theta_4 = \cos^{-1}\left(\frac{d_{upper\_arm}^2 + d_{forearm}^2 - d^2}{2d_{upper\_arm}\, d_{forearm}}\right)$ (3.18)

Then from equation (3.11) we get $\theta_2$as:

$$\theta_2 = \cos^{-1}\left(-\frac{z_e}{d_{upper\_arm}}\right) + {}^{\pi}/_{2} \quad (3.19)$$

Then from equation (3.9) and (3.17) we get θ_1 and θ_3 as follows

$$\theta_1 = \cos^{-1}\left(\frac{x_e}{d_{upper_{arm}} \cos\theta_2}\right) - {}^{\pi}/_{2} \quad (3.20)$$

And

$$\theta_3 = \cos^{-1}\left(\frac{z_w + d_{upper_{arm}} \sin\theta_2 + d_{forearm} \cos\theta_4 \sin\theta_2}{d_{forearm} \cos\theta_2 \sin\theta_4}\right) \quad (3.21)$$

By using equation (3.18), (3.19), (3.20) and (3.21) we got all four joint angle.

However, solving this inverse kinematics equations generate singularity effect specially if $\theta_2$or $\theta_4$any of them goes to zero degree position then θ_1 and θ_3 become infinity. Solving this singularity cause high computation and reduce the program execution performance. For the reason we found alternative geometric solution which is much easier to compute and reliable.

Geometric approach

Determination of angle $\theta_4$geometrically already discussed in previous section. Now the solution for others angle need some extra consideration.

Let's consider a vector **OA** along Z_0 axis in negative direction with unit length. Then the point A locate at (0, 0,-1) position. Now, the angle between d_{upper_arm} vectors **OA** is angleθ_2. Also, consider a vector **OB** along X_0 axis in positive direction with unit length. Then the point B locate at (1, 0, 0) position. Therefore, the angle between **OB** and d_{upper_arm} is angleθ_2.

Then,

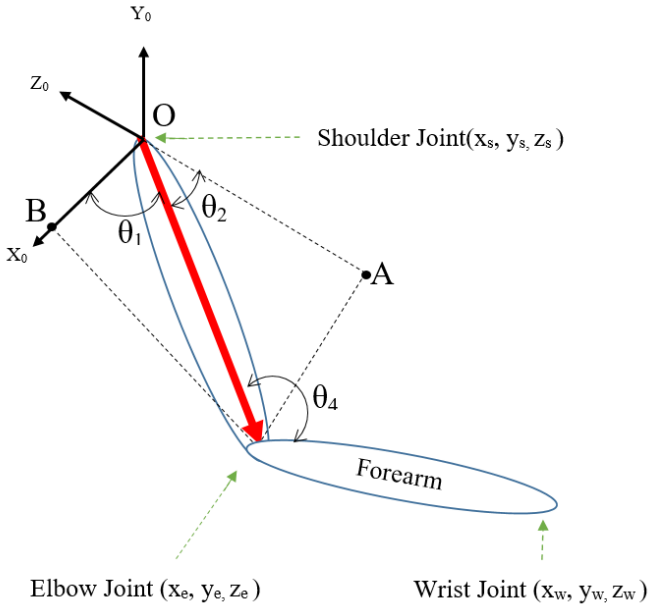

Figure 3.8 joint angle θ_1 *and* θ_4 calculation

$$\cos\theta_1 = \frac{\sqrt{(1-0)^2+(0-0)^2+(0-0)^2} + d_{upper_{arm}} - \sqrt{(x_e-1)^2+(y_e)^2+(z_e)^2}}{d_{upper_{arm}}}$$

And $\sin\theta_1 = \pm\sqrt{1-(\cos\theta_1)^2}$

Therefore, $\theta_1 = \tan^{-1}\left(\frac{\pm\sin\theta_1}{\cos\theta_1}\right)$

Similarly,

$$\cos\theta_2 = \frac{\sqrt{(0-0)^2+(0-0)^2+(-1-0)^2} + d_{upper_{arm}} - \sqrt{(x_e)^2+(y_e)^2+(z_e+1)^2}}{d_{upper_{arm}}}$$

And $\sin\theta_2 = \pm\sqrt{1-(\cos\theta_2)^2}$

Therefore, $\theta_2 = \tan^{-1}\left(\frac{\pm\sin\theta_2}{\cos\theta_2}\right)$

Finally for the θ_3 consider a plan OABC that passes through Y_0 axis and upper arm. Then the angle between this plan and forearm is θ_3.

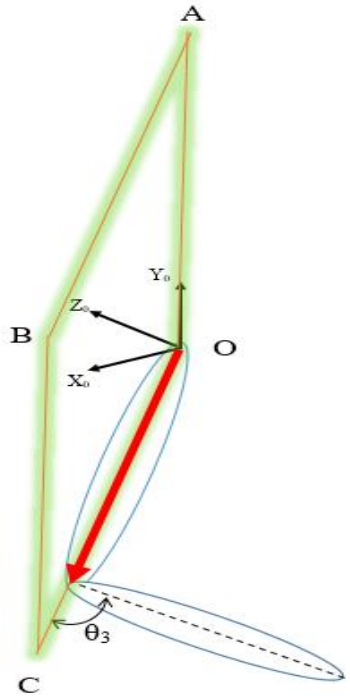

Figure 3.9 joint angle θ_3 calculation

$$\sin\theta_3 = \frac{z_e(x_{w-}x_e) - x_e(z_w - z_e)}{\sqrt{z_e^2 + x_e^2}\sqrt{(x_w - x_e)^2 + (y_w - y_e)^2 + (z_w - z_e)^2}}$$

And $\cos\theta_3 = \pm\sqrt{1 - (\sin\theta_3)^2}$

Therefore, $\theta_3 = \tan^{-1}\left(\frac{\pm\sin\theta_3}{\cos\theta_3}\right)$

All this calculations are much more simple and most reliable. It can easily take care of the singularities with some simple conditions. To match the joint angles of human with NAO robot joint orientation. It need to introduce some small change in calculation. These are

$\theta_{1,NAO,RShoulderRoll} = \theta_1 - 90°$

$\theta_{2,NAO,RShoulderPitch} = \theta_2$

$\theta_{3,NAO,RElbowYaw} = 90 - \theta_3$

And $\theta_{4,NAO,RElbowRoll} = 180 - \theta_4$

For the convenience of representation all four NAO robot joint angles are represented as $\theta_1, \theta_2, \theta_3 \; and \; \theta_4$ throughout this report.

CHAPTER 4

NAO’S REHABILITATION LIBRARY (NRL)

This chapter focuses on Aim-1. To demonstrate rehabilitation exercises with NAO, a library of recommended rehabilitation exercises involving shoulder and elbow joint movements (2011) was formed in Choregraphe (graphical programming interface) (Group 2013). In experiments, NAO was maneuvered to instruct and demonstrate the exercises from the NRL. The first section of this chapter briefly describes the Choregraphe programming interface. In the mid sections of the chapter, experimental results with NAO are presented. The chapter ends with a brief discussion on the experimental results.

4.1 Choregraphe

Choregraphe is high level programming interface for NAO robot. It provides different robot functionality as blocks (as shown in Figure 4.3). Blocks contain in a *blocks library*. Using these blocks, it is possible to build a very complex behavior for NAO. Choregraphe built-in blocks provide access to all sensors and actuators of NAO. In addition, bocks are used to access in NAO’s memory. It is also possible to build a new functional block in Choregraphe using programming language Python with the provided SDK. Choregraphe also provides a virtual NAO in which one can perform simulation of created behaviors. Choregraphe contains different types of blocks. Audio, vision, motion, sensing etc.

Figure 4.3 presents some commonly used functional blocks in Choregraphe. Audio blocks as shown in Figure 4.3(a) have some specific functionality. For instance, using the ‘Say’ block a program can be made so that NAO can speak the *text* contained in the ‘Say’ block. Figure 4.3(b) contains some basic motion blocks by which NAO can move in any direction, can sit or stand, can

waives hands etc. Choregraphe also provides access to NAO's sensors by using the *sensing blocks library* (Figure 4.3 (c)). There has also some advanced built-in blocks in Choregraphe such as speech recognition, face recognition, learning face, detect face etc.

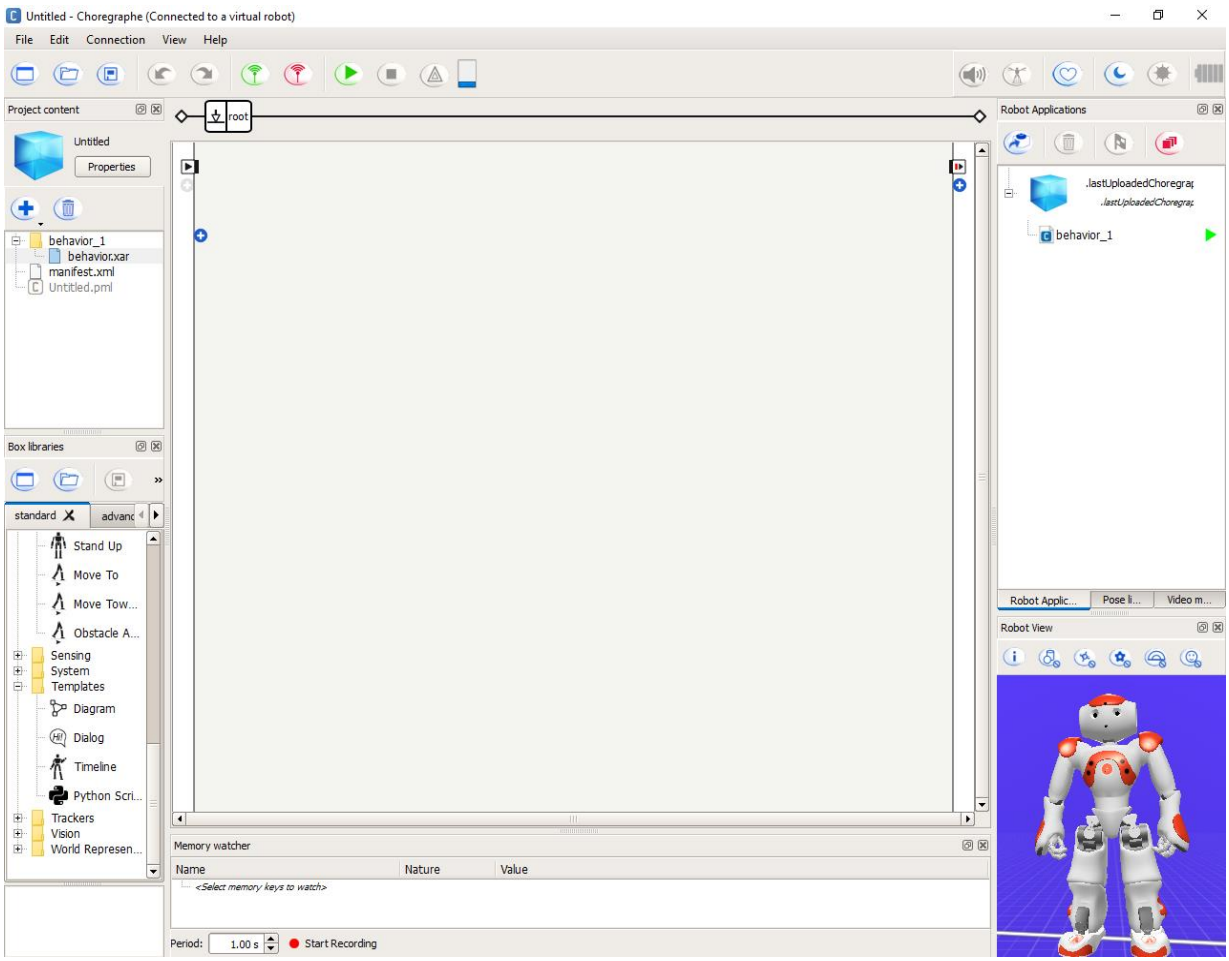

Figure 4.1 Choregraphe programming interface

Workflow in Choregraphe follows a parent child relation. Each block has input and output ports. They are connected through lines/wires and program flow in sequential order.

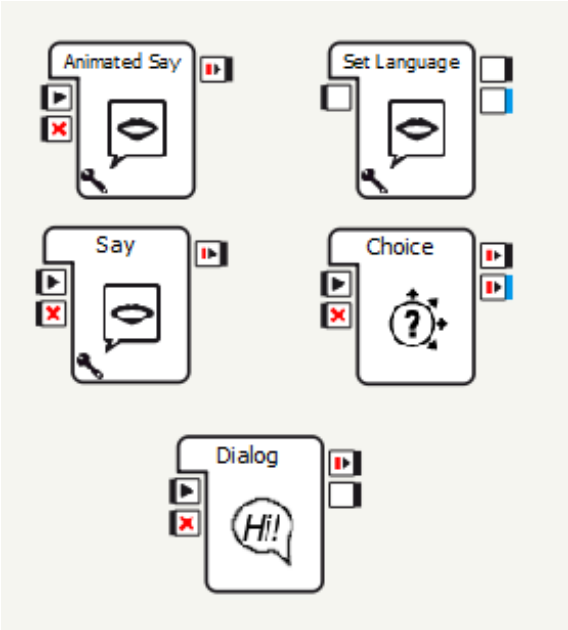

(a)

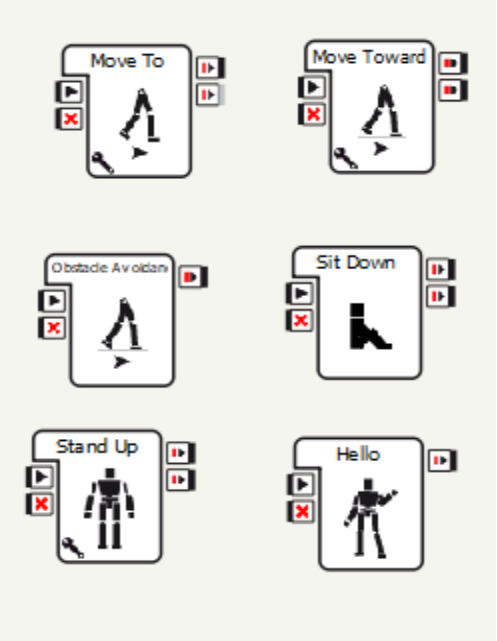

(b)

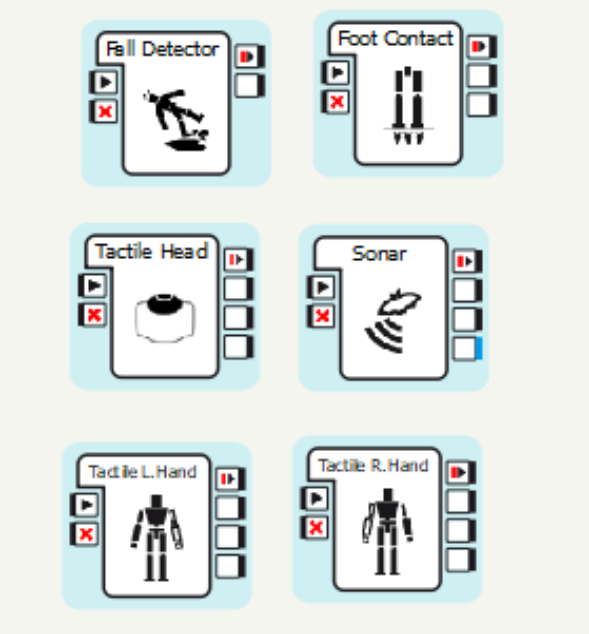

(c)

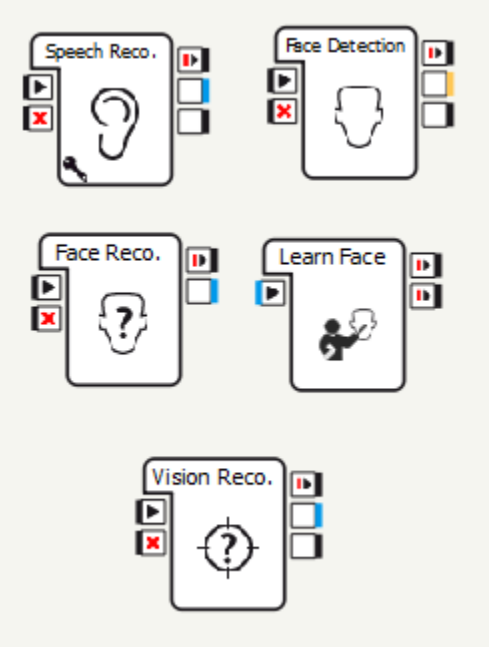

(d)

Figure 4.3 Functions blocks in Choregraphe. (a) Audio blocks, (b) Motion blocks, (c) Sensing blocks, (d) Intelligent blocks

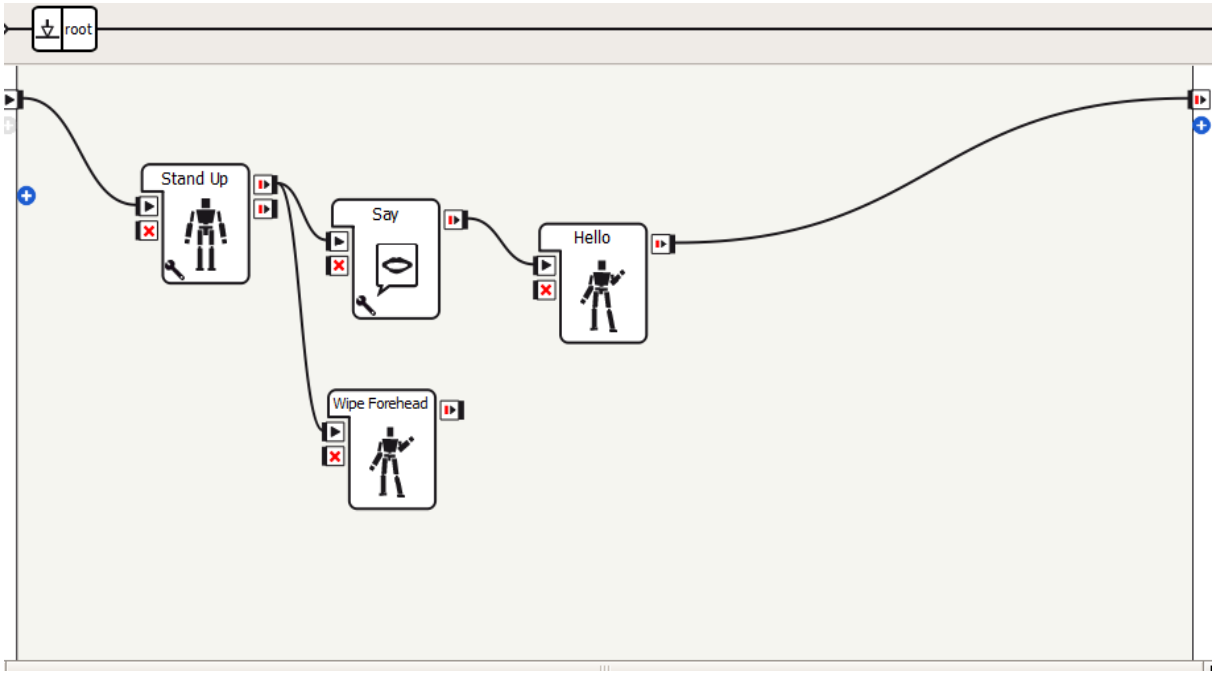

Figure 4.4 Program flow in Choregraphe

Figure 4.4 is an example of a behavior created in Choregraphe. If we execute this behavior, ‘stand up’ block (in Figure 4.4) will be executed first which will result NAO to stand-up. Then, ‘Say’ and ‘Wipe Forehead’ blocks will be executed simultaneously which will result NAO to speak and wipe his forehead simultaneously. Next, output will travel to ‘Hello’ block. This ‘Hello’ block will command NAO to say Hello and to waive his hand. Once ‘Hello’ block is executed NAO will exist the behavior.

Another important functional blocks library in Choregraphe is the ‘Timeline’ block. Using this block we can control each motor in a time frame along with executing different other functional blocks.

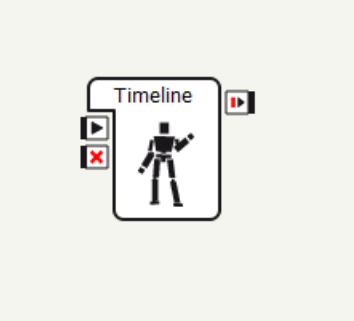

(a)

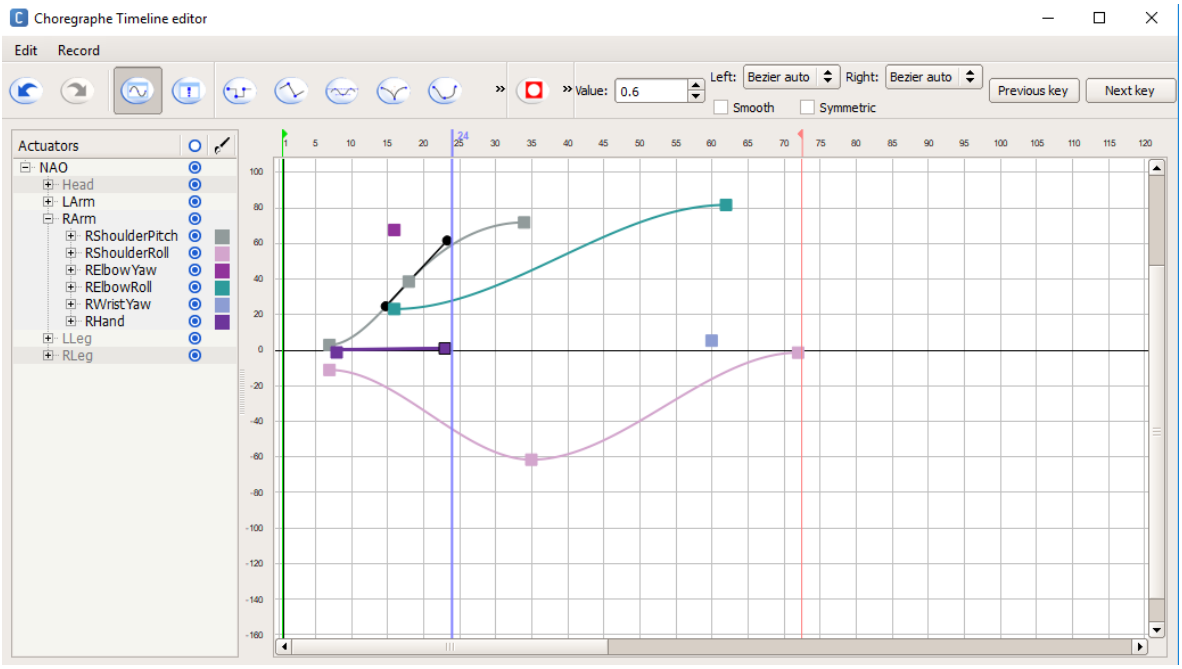

(b)

Figure 4.5 (a) Timeline block, (b) Motor trajectory control inside the timeline block

Through this timeline block, we generated joint trajectory for different types of motion exercises and set those in a library. In next section, different joint trajectories representing single and multi-joint movement rehabilitation exercises are presented. Choregraphe also provides some flow control blocks such as conditional statement blocks ‘if-else’, ’for loop’, ‘switch’ etc. These conditional blocks are used to generate a cooperative rehabilitation exercise library which is presented in section 4.2.3.

4.2 NAO's Rehabilitation Library (NRL)

The exercises formed in NRL can be grouped under three categories; 'single joint movement', 'multi joint movements', and 'co-operative exercise'. NAO will instruct and demonstrate subjects to perform those exercises. A typical NAO's instruction is given below:

{

NAO: Hello friend,

NAO: Let's get ready. Stay normal and don't worry. I am here for you mate. Believe me it's going to be fun.

NAO: Anyway, we will do some exercise together

NAO: In this session, I will show you how to do elbow flexion/extension exercise in a minute. After that you will be asked to do perform the exercise…

⋮

}

4.2.1 Single joint movements

Single joint movement exercises in NRL include shoulder joint abduction/adduction, shoulder joint vertical flexion/extension, shoulder joint internal/external rotation, and elbow joint flexion/extension motion. Since NAO does not have wrist joint flexion/extension and radial/ulnar deviation we have excluded wrist joint motions from this study.

- **Shoulder joint movements**

  Figure 4.6 shows the experimental results of shoulder joint abduction/adduction where a coordinated movement of shoulder horizontal and vertical flexion/extension motion were

performed. The top plot of Figure 4.6 shows NAO's abduction/adduction angle as a function of time. The bottom plot of Figure 4.6 shows the joint velocity. As shown in Figure 4.6 and

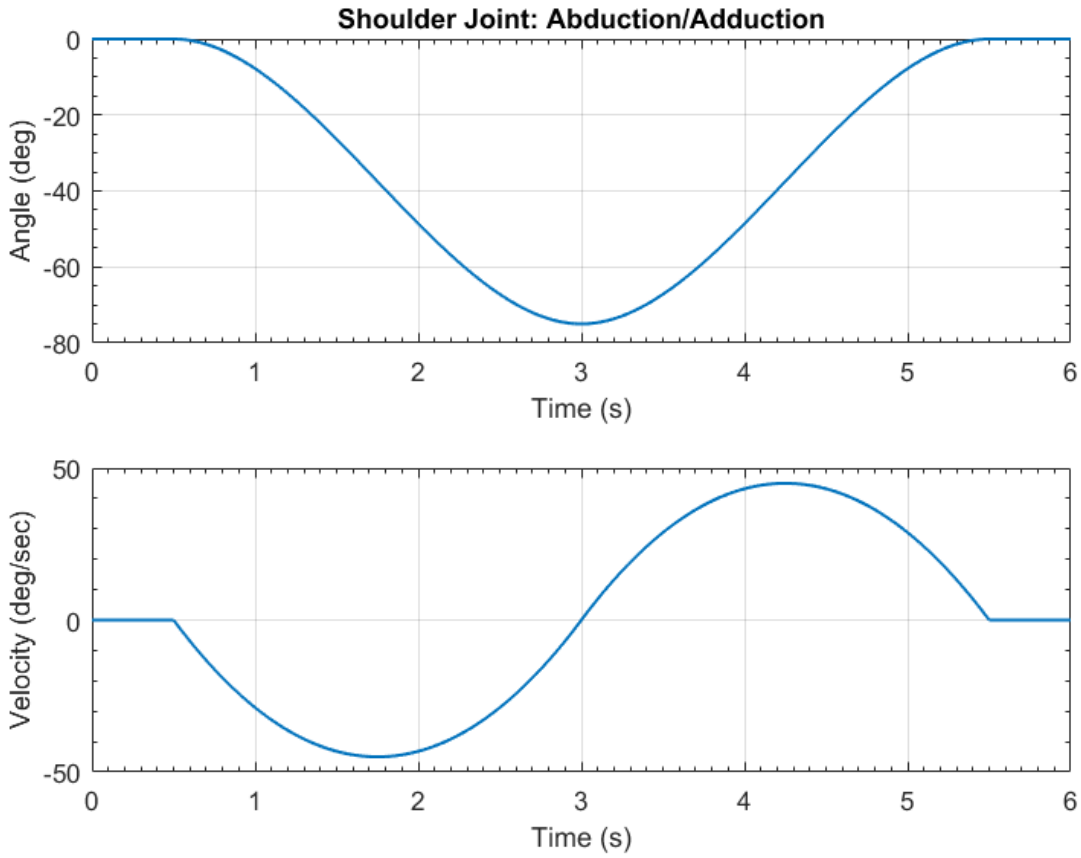

Figure 4.6 Shoulder joint abduction/adduction motion (joint trajectory and velocity)

Figure 4.7 (a), the exercise began with NAO's adduction angle 0° then abduction motion was performed (Figure 4.7 (e)), finally the exercise ends with the NAO's adduction to 0° (Figure 4.7 (a)). Maximum abduction angle observed in this case was -75°.

A typical rehabilitation exercise involving shoulder joint flexion/extension movement is depicted in Figure 4.8 and Figure 4.9 where the NAO raises its arm (from the initial position, i.e., shoulder joint-2 is at 90°) straight up to a specific position over the head (e.g., in 4.8 (e),

the elevation was set to a range of 180°, i.e., from 90° to -90°) and then slowly moves the joint back to its initial position.

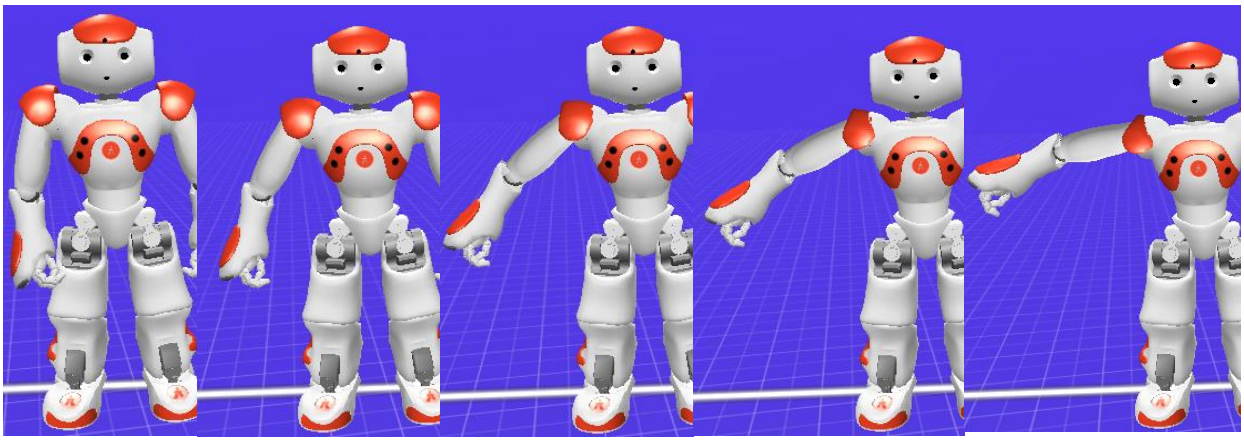

(a) (b) (c) (d) (e)

Figure 4.7 Abduction/adduction motion of NAO

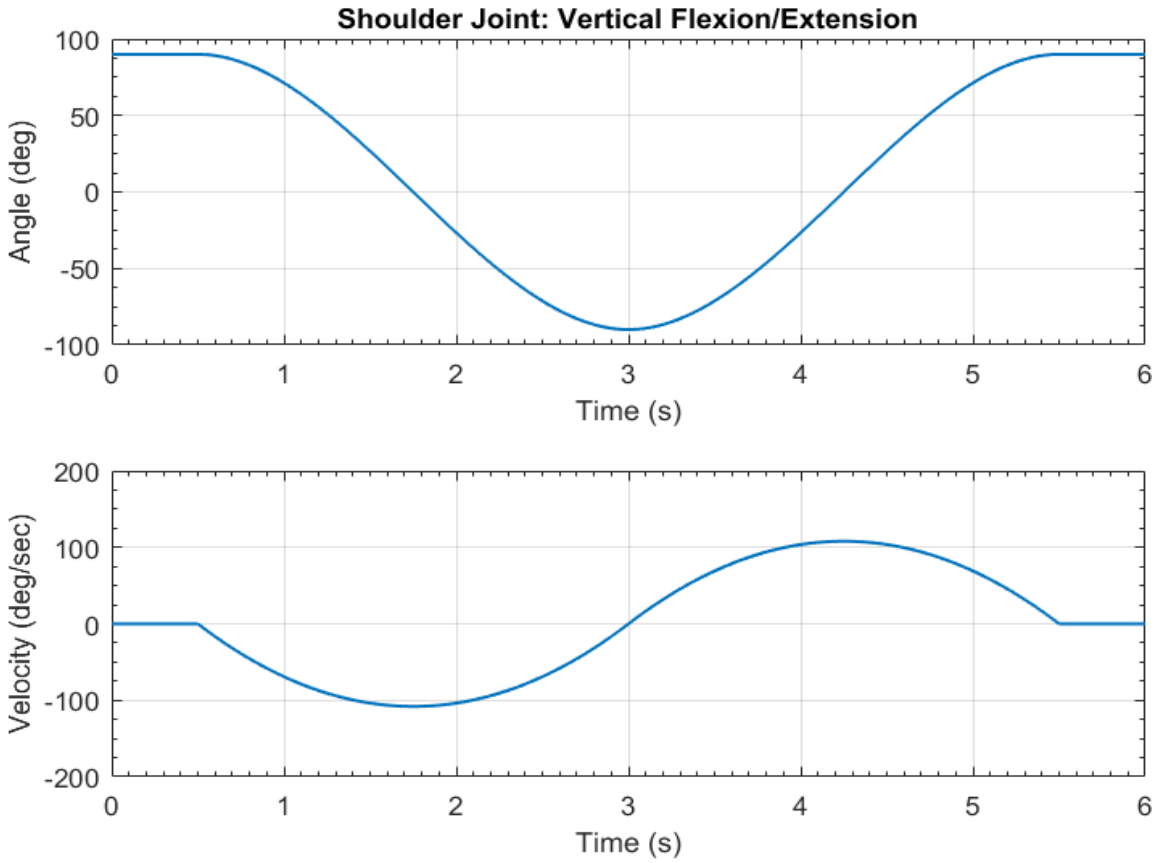

Figure 4.8 Shoulder joint vertical flexion/extension motion (joint trajectory and velocity)

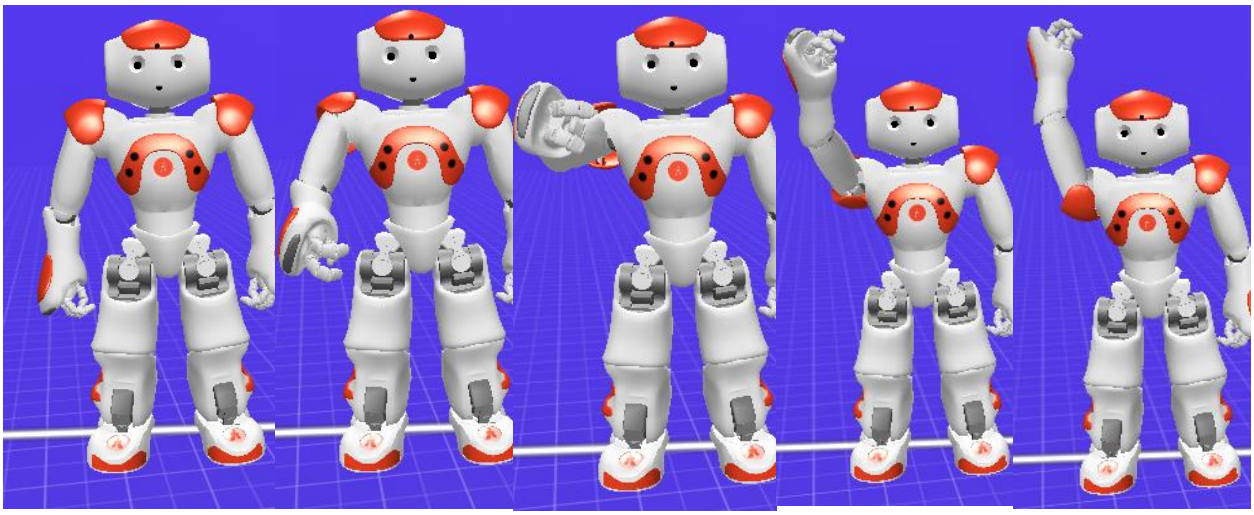

(a) (b) (c) (d) (e)

Figure 4.9 Shoulder flexion/extension motion of NAO.

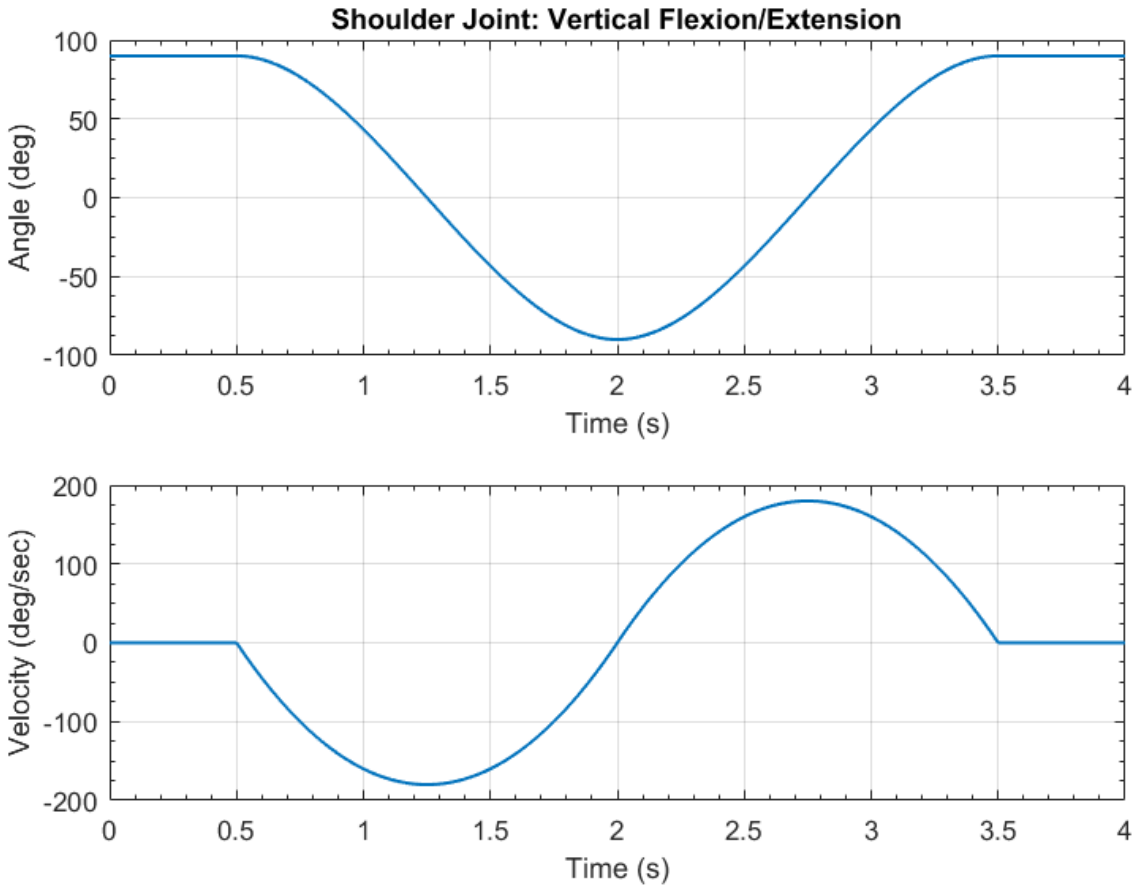

Figure 4.10 Shoulder joint vertical flexion/extension motion (fast movement)

Depending on the subject, it is often required to change the speed of such exercises. Figure 4.10 shows the similar exercises that were performed with different speeds of motion.

Figure 4.11 and Figure 4.12 demonstrate a co-operative movement of the elbow (flexion/ extension) and shoulder joint (internal/external rotation). The objective of this exercise is to demonstrate shoulder joint internal/external rotation while maintaining the elbow at 90°. As shown in Figure 4.12 (a), the exercise begins with elbow flexion at 90°, then internal/external rotation was performed (Figure 4.12).

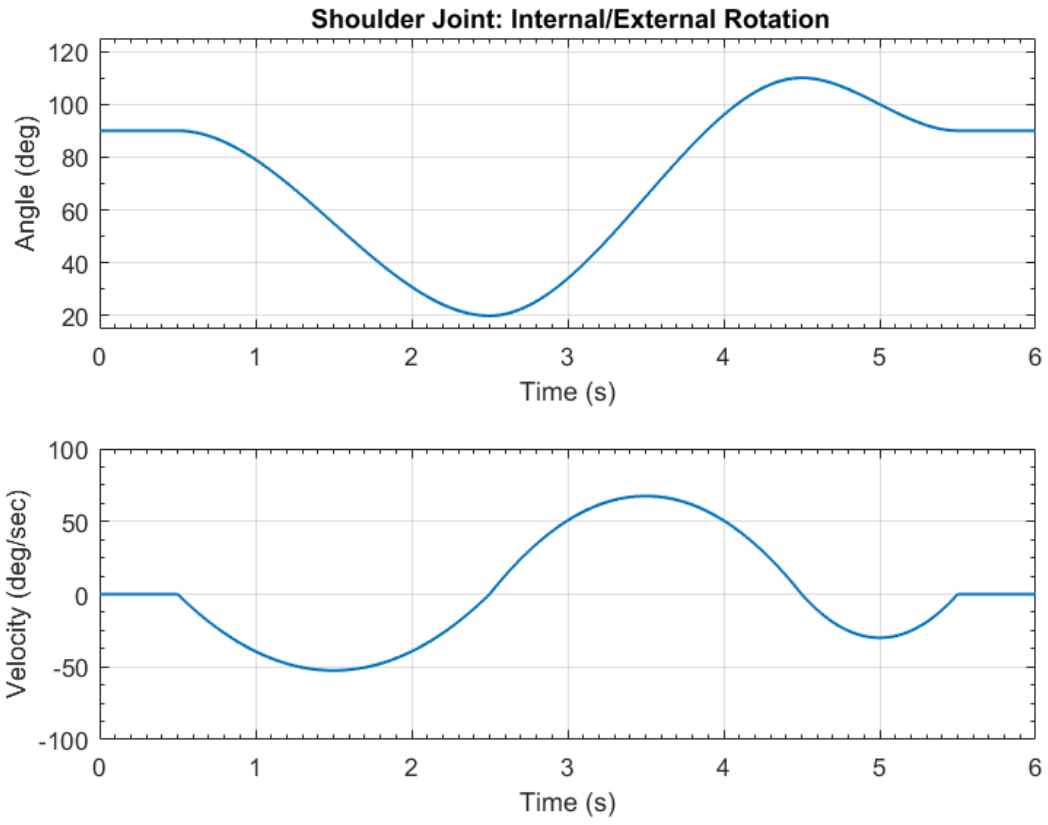

Figure 4.11 Shoulder joint internal/external rotation (joint trajectory and velocity)

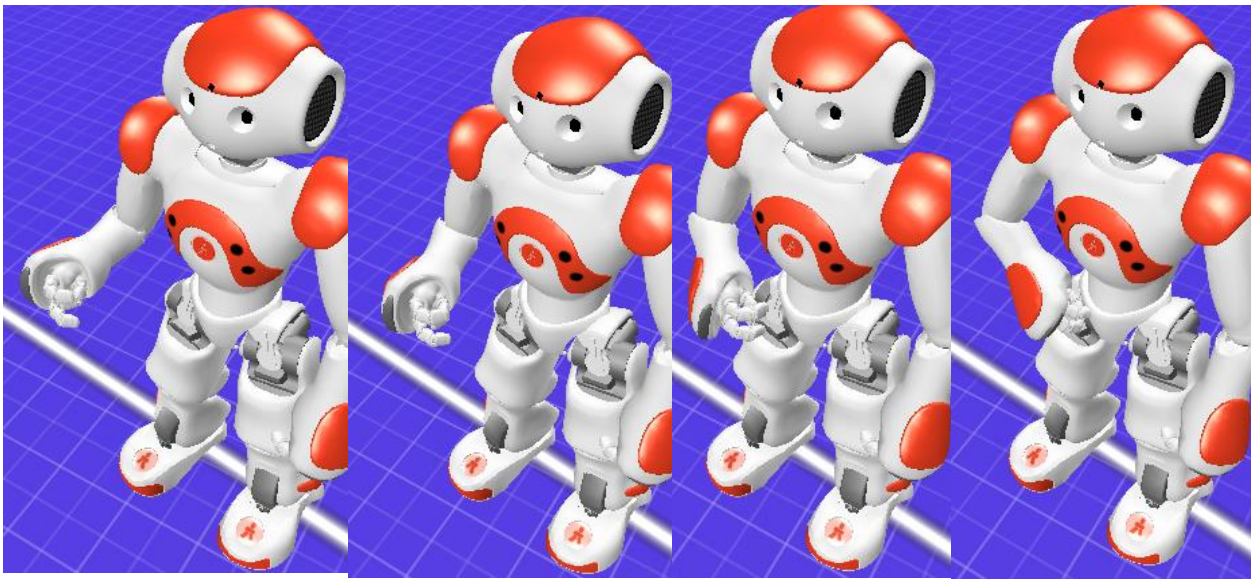

(a) (b) (c) (d)

Figure 4.12 Shoulder joint internal/external rotation of NAO. (a) Elbow joint at ~90º, (b-d) internal/external rotation

- **Elbow joint movements**

  A typical rehabilitation exercise involving elbow joint flexion/extension movement is depicted in Figure .4.14 and Figure 4.12.The exercise began with the elbow joint at 4° and then a repetitive flexion/extension motions were performed.

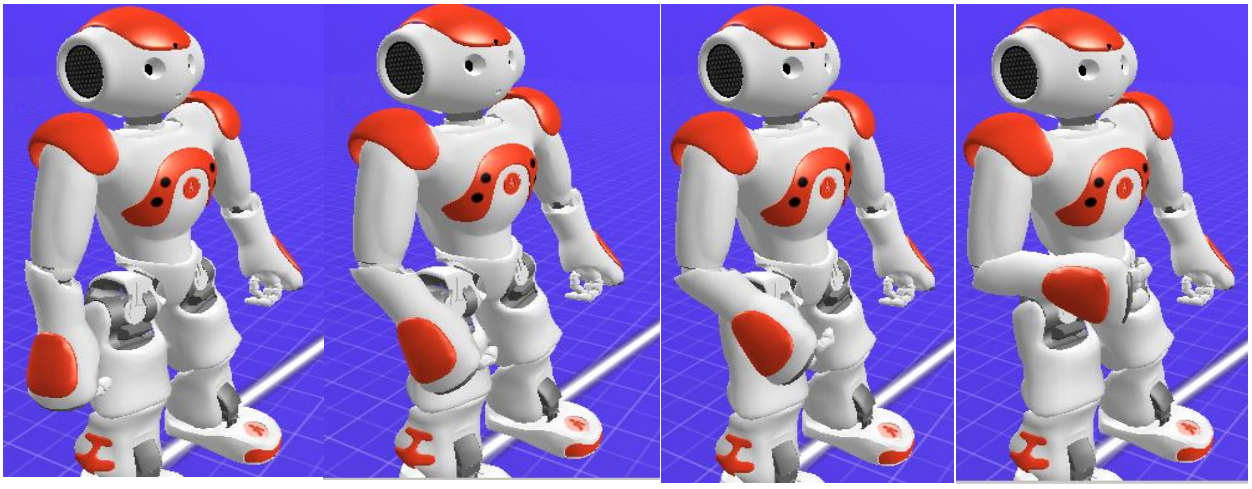

(a) (b) (c) (d)

Figure 4.13 Elbow joint flexion/extension of NAO

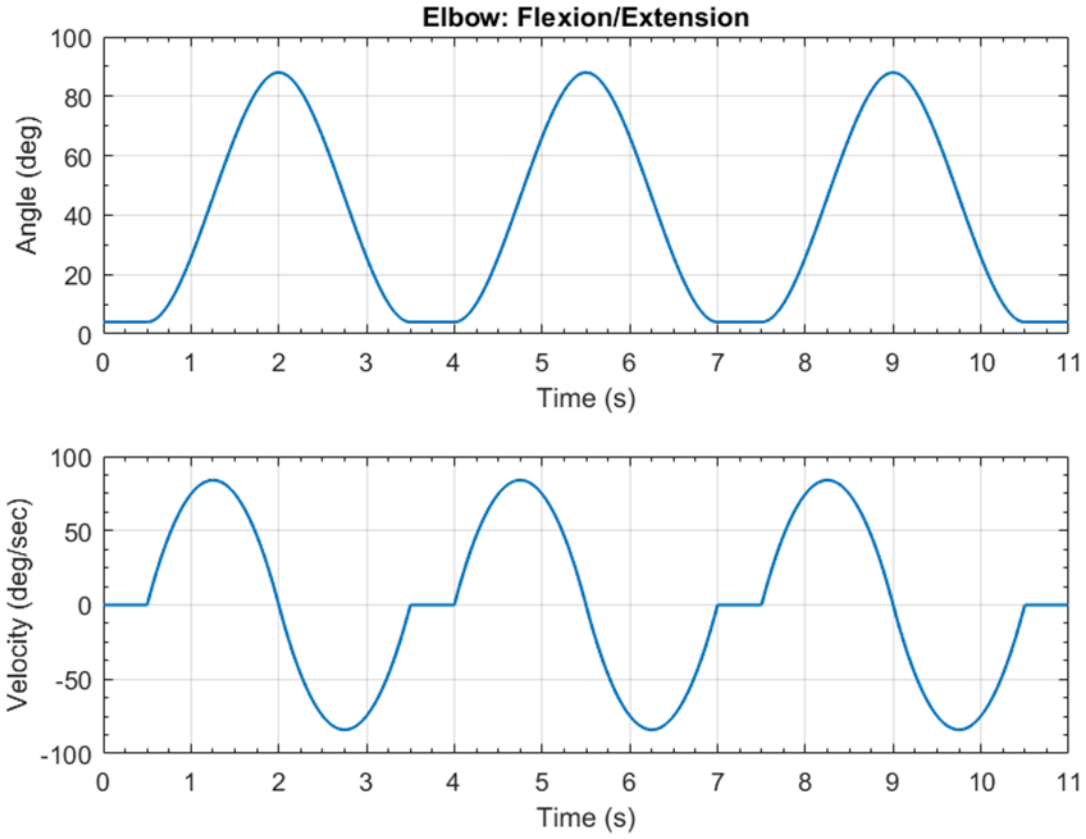

Figure .4.14 Elbow joint flexion/extension (joint trajectory and velocity)

4.2.2 Multi joint movements

Multi joint movement exercises in NRL include a combination and co-operative movements of shoulder joint (abduction/adduction, vertical flexion/extension, internal/external rotation), and elbow joint (flexion/extension) motion.

- **Reaching movements**

Reaching movements are widely used and recommended for multi joint movement exercises. A forward reaching movement and a diagonal reaching movement exercise is depicted in Figure 4.15 and in Figure 4.17 respectively.

Forward reaching movement involves shoulder joint flexion/extension motion and elbow joint flexion/extension motion. Experimental results of forward reaching movement showing the elbow and shoulder joint angles are illustrated in Figure 4.14.

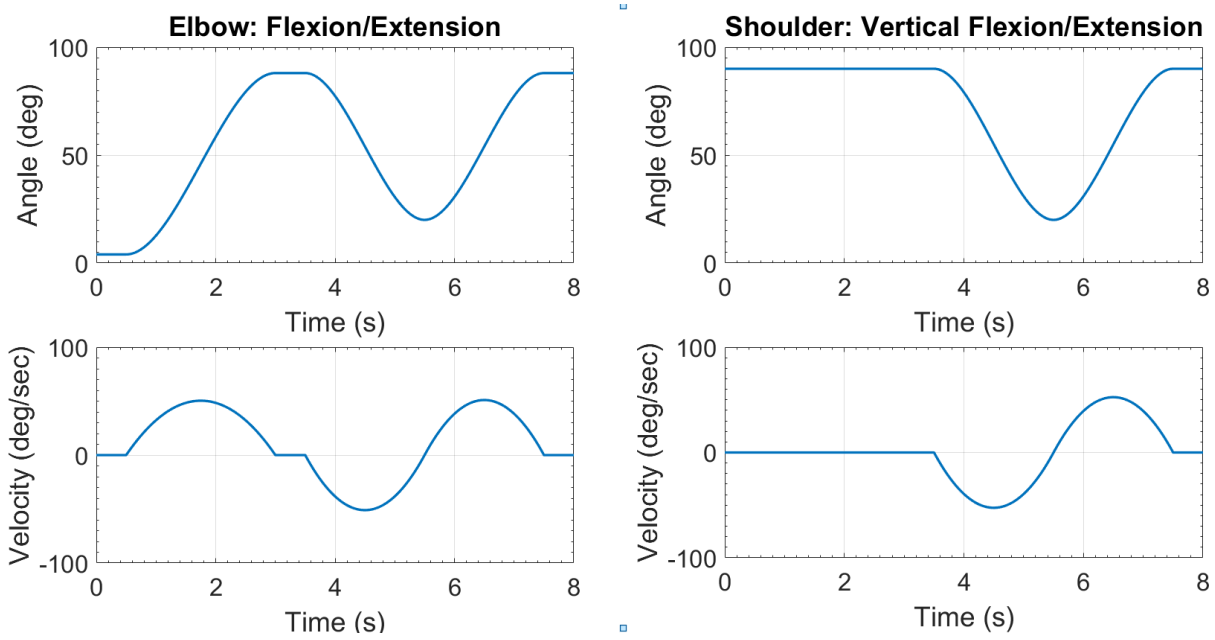

Figure 4.15 Reaching movements (forward)

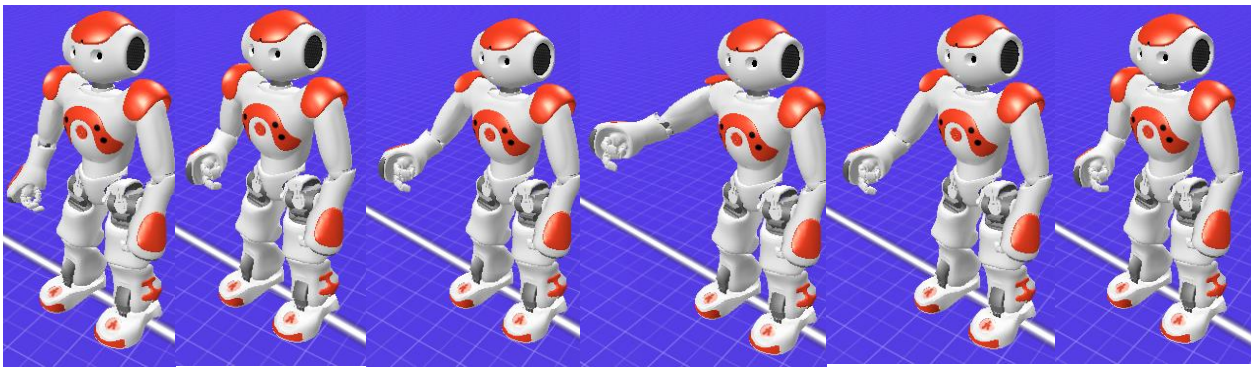

(a) (b) (c) (d) (e) (f)

Figure 4.16 Forward reaching movements performed/demonstrated by NAO

Diagonal reaching movement involves shoulder joint flexion/extension motion, shoulder joint abduction/adduction, and elbow joint flexion/extension motion. Experimental results of diagonal reaching movement showing the elbow and shoulder joint angles are illustrated in Figure 4.16. Typically this exercise is repeated approximately 10 times (Physical therapy Standard, 2011) therefore a few repetitions are depicted in Figure 4.16. NAO will instruct the subjects to perform a repetitive motion of this exercise.

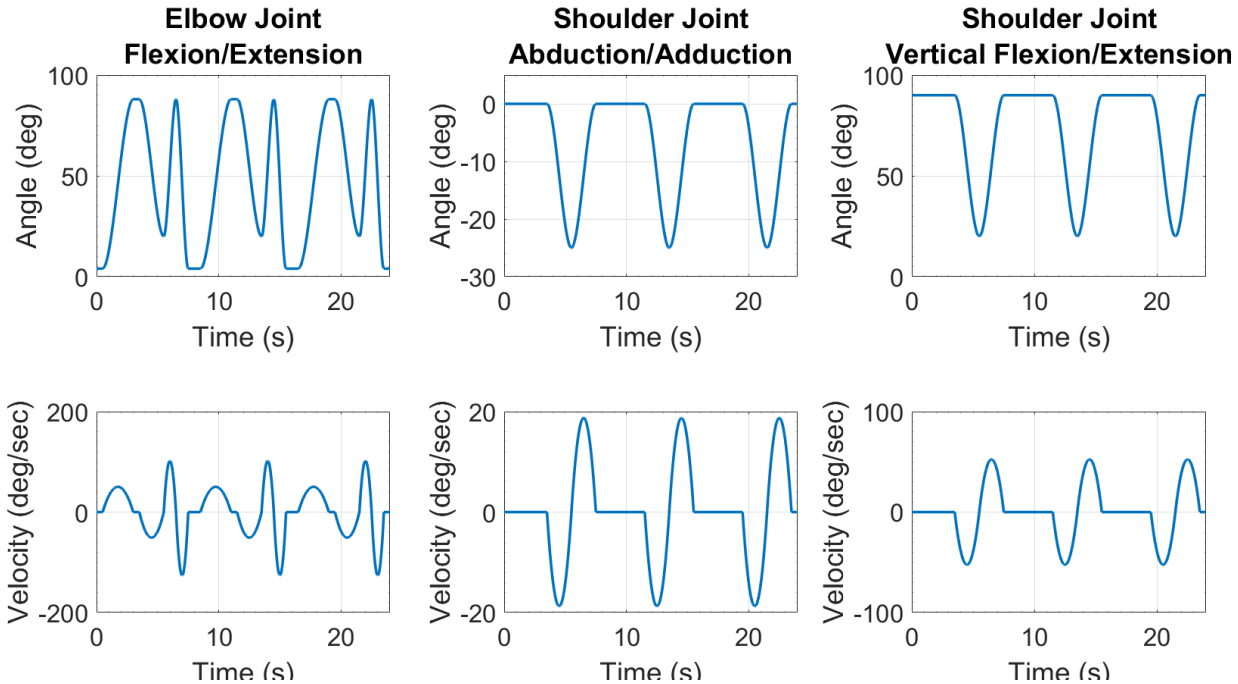

Figure 4.17 Diagonal reaching movements

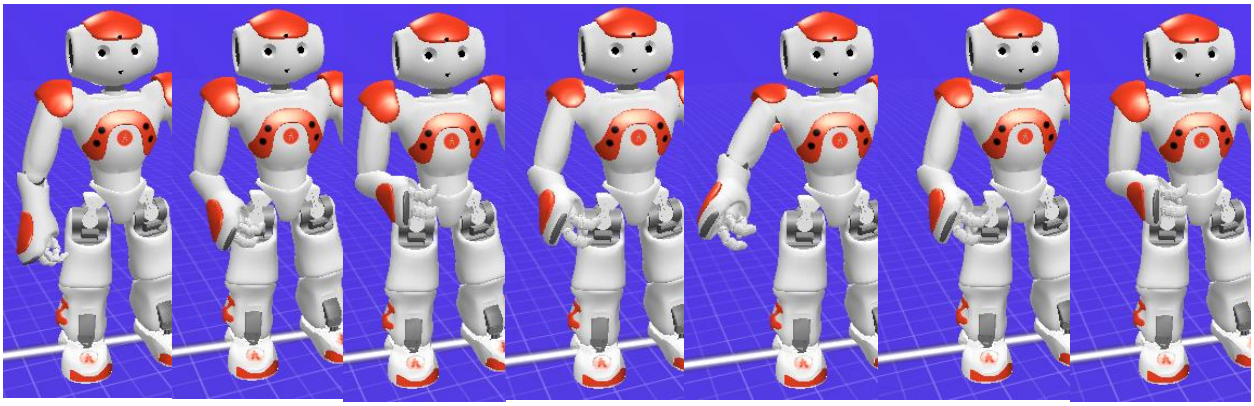

(a) (b) (c) (d) (e) (f) (g)

Figure 4.18 Diagonal reaching movements performed/demonstrated by NAO

4.2.3 Cooperative exercise

Cooperative exercises in NRL involves NAO's interaction with subjects. Figure 4.19 shows the schematic diagram of a cooperative exercise 'touch and play' where points A, B, C, D represents NAO's hand position in 3D space at different time. The objective of this exercise is to reach different targets one after another which involve movement of the entire upper limb's joints. Figure 4.20 shows few snapshots while NAO was playing 'touch and play' game with the subject. Experiments were conducted with a healthy subject in seated position (Figure 4.20a). In this experiment NAO instruct the subject to touch his hand in a 3D space (e.g, point A, Figure 4.20b). When the subject touches NAO's hand he can sense it with his tactile sensor, move his hand at a new position, and ask the subject to touch his hand again.

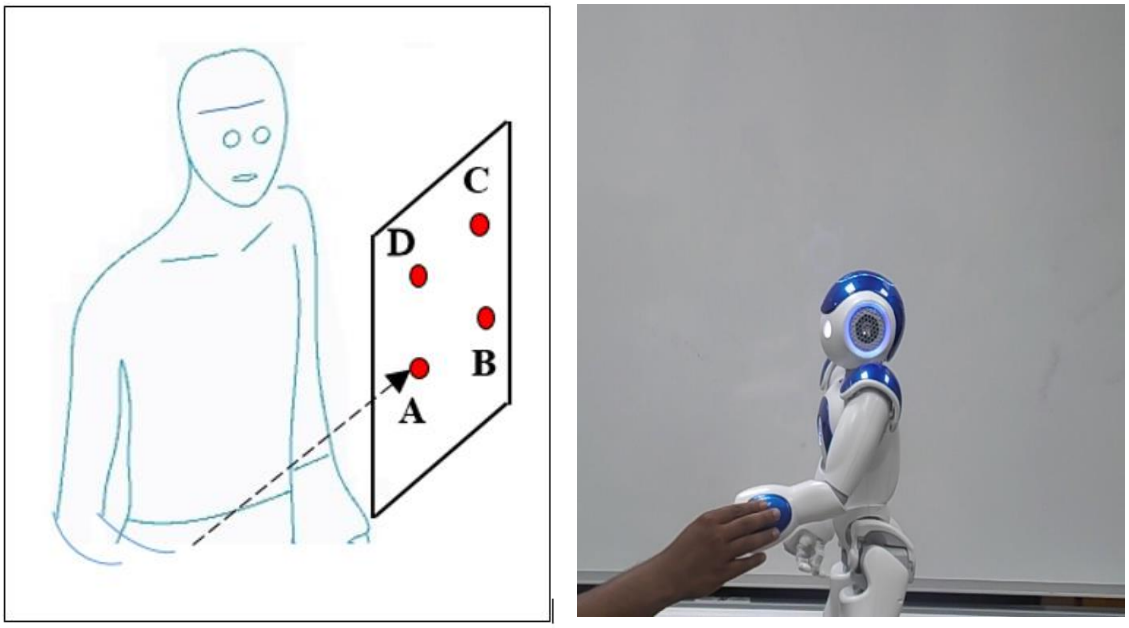

Figure 4.19 Schematic of 'touch and play' exercise

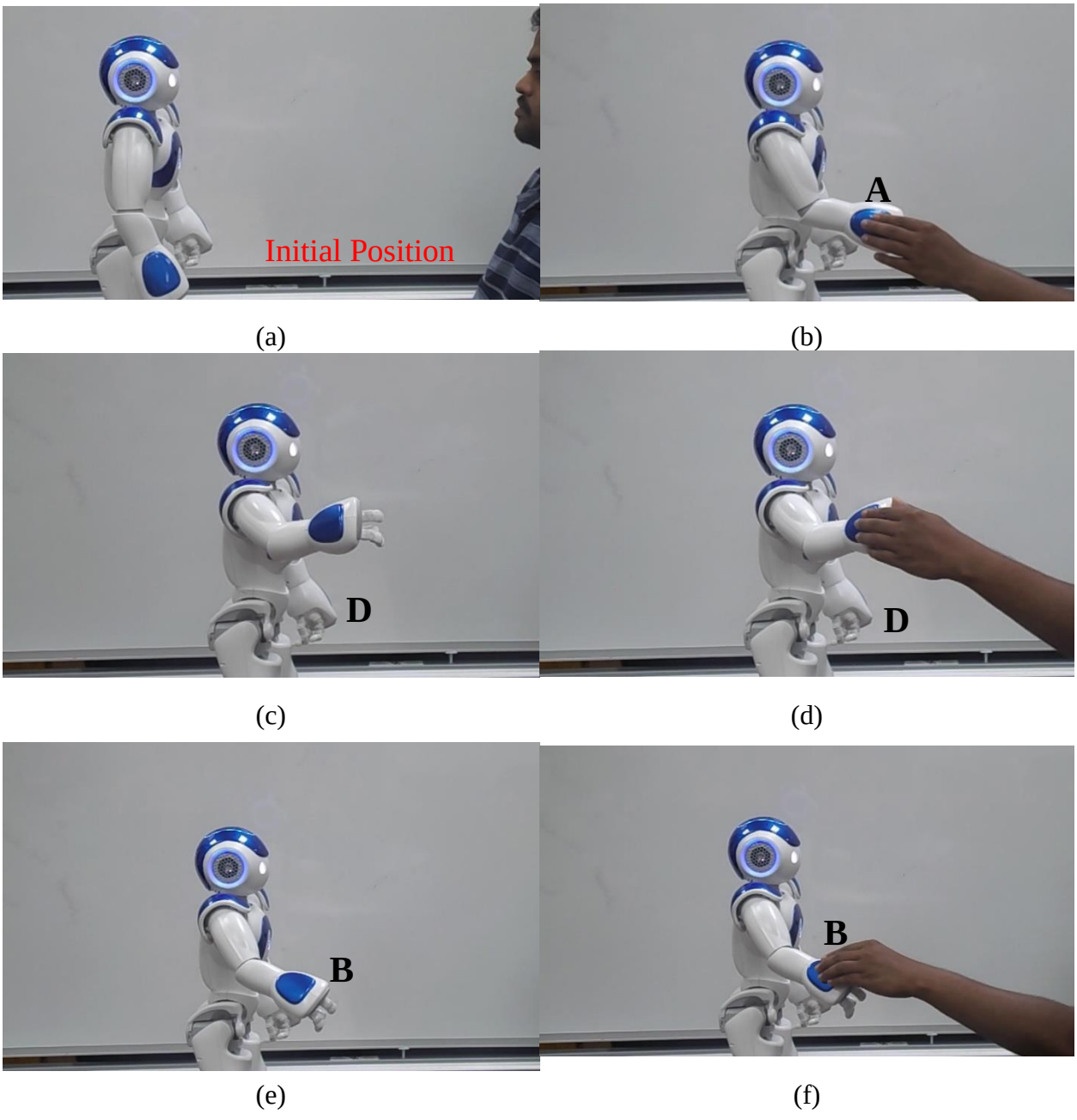

(a) (b)

(c) (d)

(e) (f)

Figure 4.20 Cooperative exercise with NAO robot

Finally, to perform more complex cooperative exercises with NAO, we combined all the functional behaviors (single joint movement exercises, multi join movement exercise, co-operative

movement exercise) described in sections 4.2.1 to 4.2.3. A sample of such cooperative exercise (developed in Choregraphe) is shown in Figure 4.21.

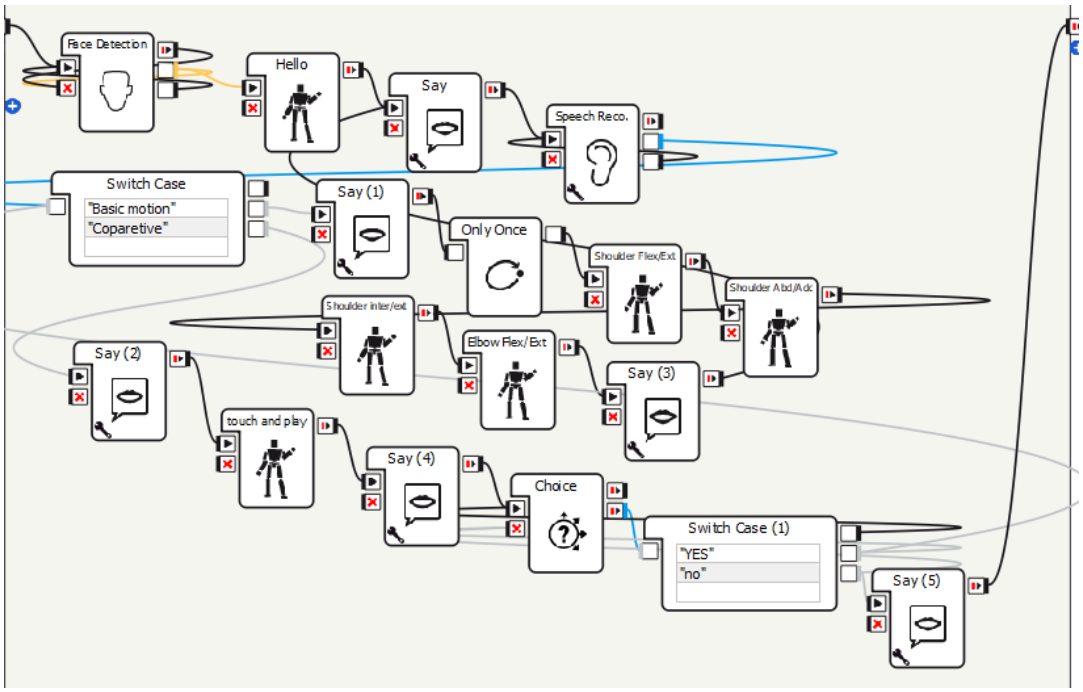

Figure 4.21 NAO's behavior programming for single and multi-joints movements and cooperative tasks

Pseudocode: Flow of robot functionality for behavior in Figure 5.20

```
Trigger
Detect face
If face>1
Say → greetings
Ask*→ exercise type
Speech recognition← say type
        If basic motion = true
                Say & execute: consecutive basic motion
                If finish
                   ask→repet→"yes"|| "no"
                   if yes=true
                       Goto Ask*
                   if no= true
                      exit behaviour

        else If cooparetive = true
```

```
Ask**→touch hand
hand tactile←yes
move→new position
if finish
   ask→repet→"yes"|| "no"
   if yes=true
      Goto Ask**
   if no= true
      exit behaviour
```

A list of NAO's rehabilitation exercise is summarized in Table4.1

Table 4.1 NAO's rehabilitation exercise

1. Elbow flexion/extension	2. Move hand in a rectangular path
3. Elbow rotation	4. Move hand diagonally
5. Shoulder abduction/adduction	6. Move hand in zig zag way
7. Shoulder flexion/extension	8. Touch and play
9. Shoulder horizontal flexion/extension	10. Slowly clap with my hand
11. Arm in lap	12. Touch my sensor where I can feel
13. Arm reach to head level	14. Hold my wrist
15. Arm reach to left, head level	16. Open /close your hand
17. Touch my bumper	18. Touch my bumper
19. Speed up motion continuously	

Conclusion:

Experimental results shown in sections 4.2.2 to 4.2.4 reveals that NAO can be effectively used to instruct and demonstrate upper-extremity rehabilitation exercises for single and multi-joint movements.

CHAPTER 5

TELE-REHABILITATION SCHEME

This chapter focuses on Aim-2. To develop a rehabilitation scheme that utilizes the concept of teleoperation. In the previous chapter, we built a library that contains a set of recommended rehabilitation exercises for NAO robot, which will be performed, by NAO robot later. However, what if it is required to introduce new exercise remotely? Teleoperation can be used to introduce new exercises in front of the patient and a therapist can be demonstrated different rehab exercise to different group of people at the same time remotely. Different group of people from different place can get therapy from same therapist at the same time using tele-rehabilitation scheme. Some stroke patient may not feel comfortable showing their disability to other people, or they may not feel good being in front of other people. The tele-rehabilitation is a possible solution in such a case. The first section of this chapter describes the methodology of how can NAO robot be operated remotely using Kinect sensor. The chapter ends with the performance analysis of teleoperation for NAO robot with Kinect sensor.

5.1 Methodology

To control the movement of the right arm of NAO robot remotely we used Kinect sensor to generate the control signal. As described in chapter 3 from the Kinect sensor it is possible to track human motion in front of it. The angle value obtained from the Kinect data then needs to be sent to the NAO's operating system. To send the signal to NAO robot, Python programming language was used along with Python SDK. In this case, we need to have MATLAB and Python communicating and there are several ways to do so. In this project, TCP/IP socket was used to

obtain a communication between MATLAB and Python. For this, a TCP/IP object was created in both MATLAB and Python with the same IP address and port. MATLAB sends the angle value to python through this TCP/IP object and after receiving the angel value Python sends the motor command to NAO robot by calling ALmotion modules in NAOqi. Then NAOqi sends the control signal to the NAO joint motor. NAOqi uses linear interpolation method to generate the motion trajectory between two successive motor commands.

Algorithm to track human motion and send signal to python in MATLAB

Call **MAX function to call C++ function(for utilizing Kinect SDK)**
Create **kinect object**
Create **TCP/IP object**
While **true**
    Call **body index frame from Kinect SDK**
    If**(number of body>1)**
        Call depth frame(from Kinect.SDK)
        Track joint
        Calculate angle value
        Send angel value to python
    End
    If**(Press q)**
      Break
    End
End
Destroy **tcp.ip object**
Destroy **Kinect object**

Algorithm to receive signal from MATLAB and send command to NAO robot in Python

Create motion proxy for NAO
Create TCP/IP object
Create communication

```
If connection = true
    While true
        Receive angle data
        If data=true
            Call motion proxy
            Send motor command
        If data = false
            Break
Destroy connection
```

5.2 Performance analysis

To analyse the performance of teleoperation, we conducted some basic experiments on NAO robot. In front of Kinect sensor, four single joint motion: i) shoulder abduction adduction (NAO robot RShoulderRoll,θ_1), ii)shoulder vertical flexion extension(NAO robot RShoulderPitch, θ_2), iii)shoulder internal external rotation(NAO robot RElbowYaw, θ_3) and iv)elbow flexion extension(NAO robot RElbowRoll, θ_4) were performed by human that was mimic by NAO robot real time. The experimental result is shown below.

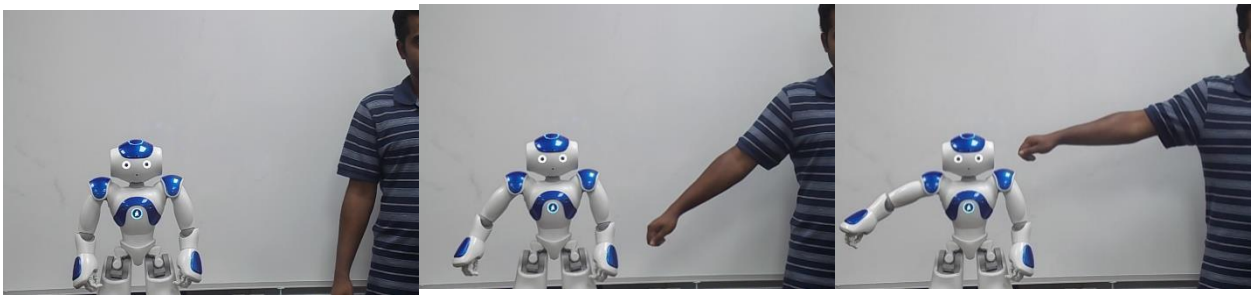

Figure 5.1 Arm position of the human operator and NAO robot during shoulder joint abduction/adduction teleoperation.

In our first teleoperation experiment, NAO robot's shoulder abduction/adduction motion was controlled. In Figure 5.1 shows the position of upper arm of NAO robot and human operator at

different times of shoulder abduction/adduction motion. Motion start from -10^{o} and end at -74^{o} because which in the range of NAO's motion.

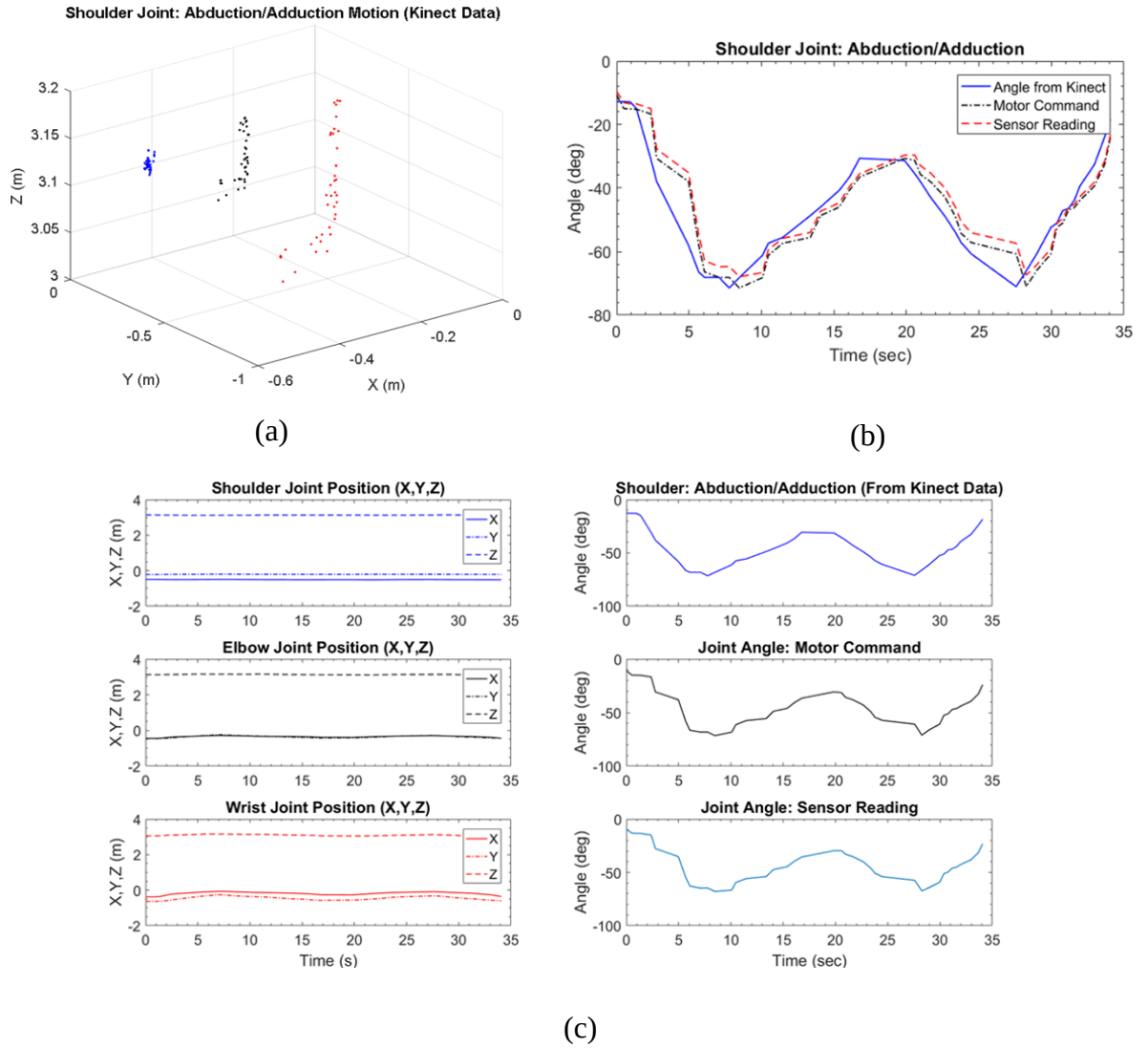

Figure 5.2 Shoulder joint abduction/adduction teleoperation. (a) Joint coordinate from Kinect (b) comparison between joint angles from Kinect and NAO robot.(c) coordinate data and joint angles from Kinect and NAO robot.

Figures 5.2 (a) and (c) shows the coordinate data of joints obtained from Kinect sensor for shoulder, elbow and wrist joint .For shoulder abduction/ adduction joint motion, Z coordinate form

Kinect frame for all joint should be constant which is match with the tracked result. Figures 5.2 (b) and (c) display the trajectory followed by human operator and NAO robot. We obtained the motor position feedback from NAO robot through Device Communication Manager (DCM). There are to separate reading comes from NAO robot DCM one reading that comes from motor controller output that goes to the motor for execution which is called motor command and other reading comes from the Joint position sensor MRE (Magnetic Rotary Encoders) which is called sensor reading. From the (b) it is clearly seen that there are some difference between this two reading. This is because when NAO robot move any joint the motion is interpolated between current value of motor position and the targeted value and it takes some time for the command to go to the motor cards and take some time for sending the reading back. There is also some laggings between Kinect value and motor command because these two programs are in two different platform Kinect extract data in MATLAB and Python communicate with NAO robot through wifi communication. MATLAB and Python communicate through tcp/ip communication. There is some delay between sending and receiving data between MATLAB and Python. In addition, NAO robot need some time to execute all its current command to take next command. To eliminate this all the platforms are needed to be synchronized. However, it is a little bit difficult when there more than three platforms being used (in this case MATLAB, Python, NAOqi). Nevertheless, from figures it is clear that the pattern of joint trajectory followed by NAO robot is exactly similar to the operator trajectory pattern.

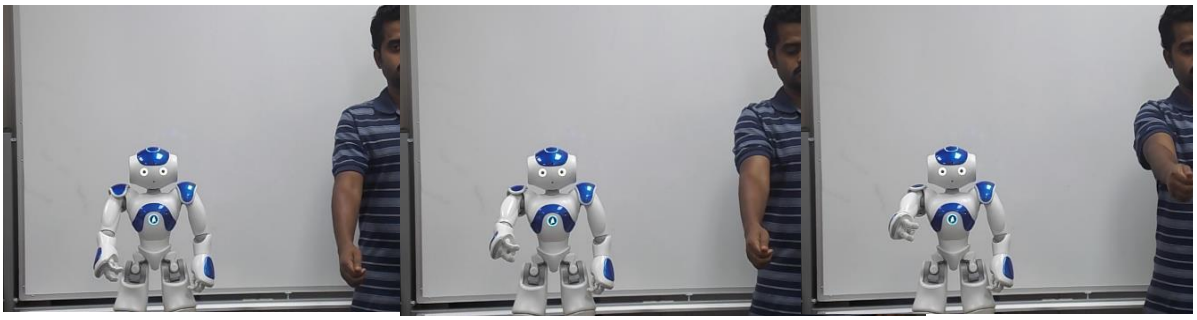

Figure 5.3 Arm position of human operator and NAO robot during shoulder joint vertical flexion/extension teleoperation

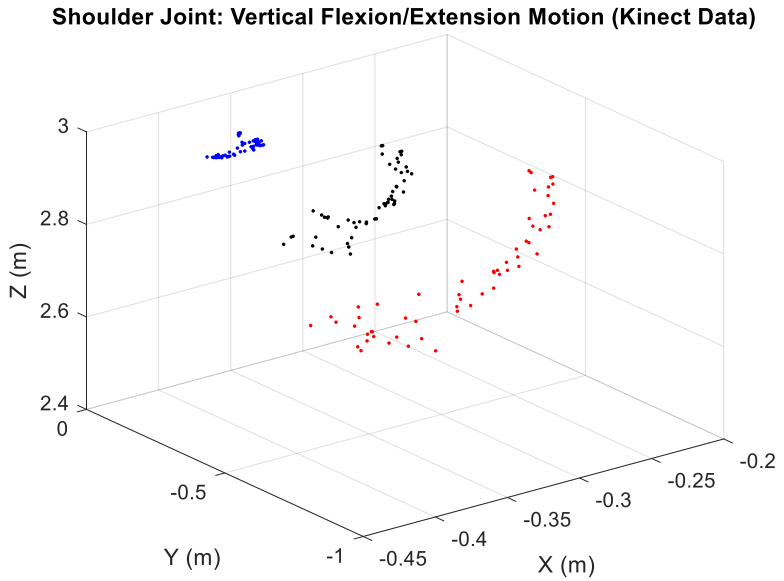

Figure 5.4 (a) Shoulder joint flexion/extension teleoperation, (joint coordinate from Kinect)

Figure 5.1 shows the upper arm position of NAO robot and human operator at different times of shoulder joint vertical flexion/extension motion. Motion start from 90 degree and end at 15 degree. Actual range for this motion is higher than 90 to 15 degree, but we limit this motion 90 to 0 degree for experimental purpose.

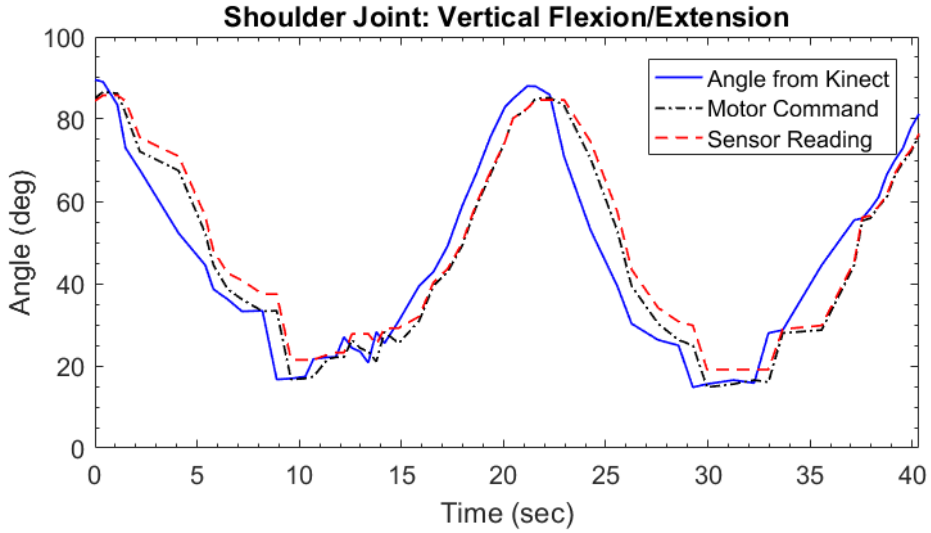

(b)

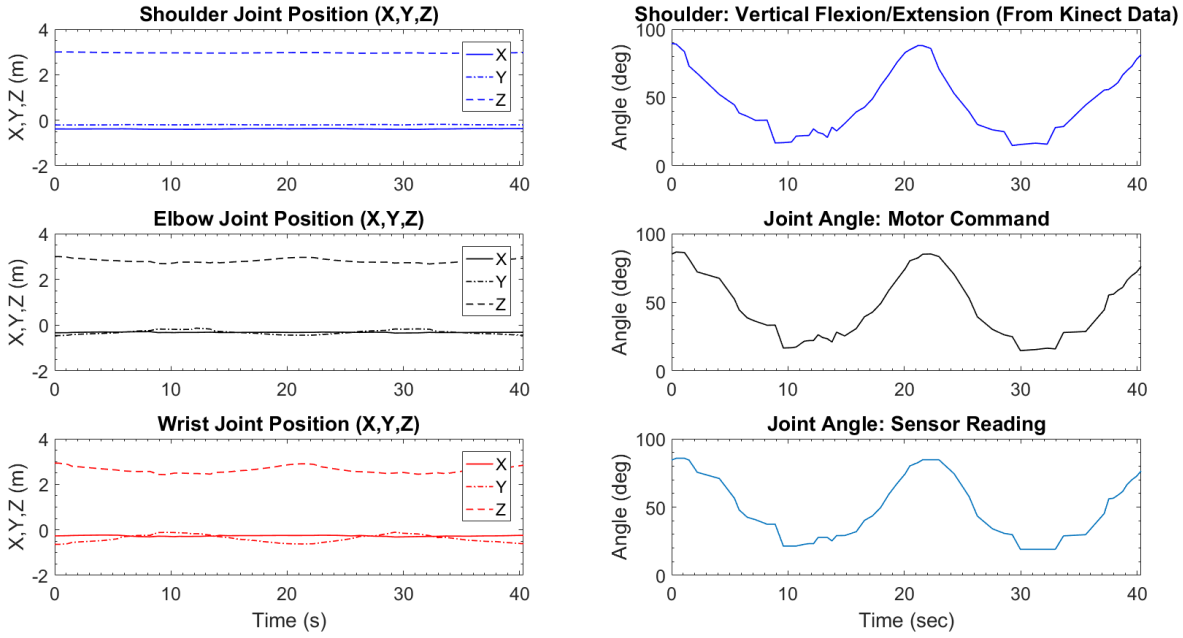

(c)

Figure 5.4 Shoulder joint flexion/extension teleoperation. (b) comparison between joint angles from Kinect and NAO robot.(c) coordinate data and joint angles from Kinect and NAO robot.

Figure 5.5 (a) and (c) shows the coordinate data obtained from Kinect sensor for shoulder, elbow and wrist joint .For shoulder vertical flexion/extension joint motion X coordinate form Kinect frame for all joint should be constant which is match with the tracked result. Figure 5.5 (b) and (c) display the trajectory followed by human operator and NAO robot.

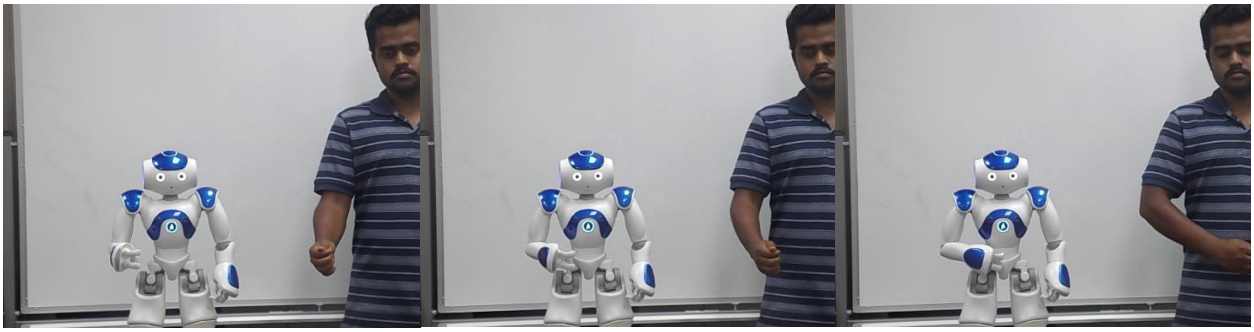

Figure 5.5 Arm position of human operator and NAO robot during shoulder joint Internal/external rotation during teleoperation

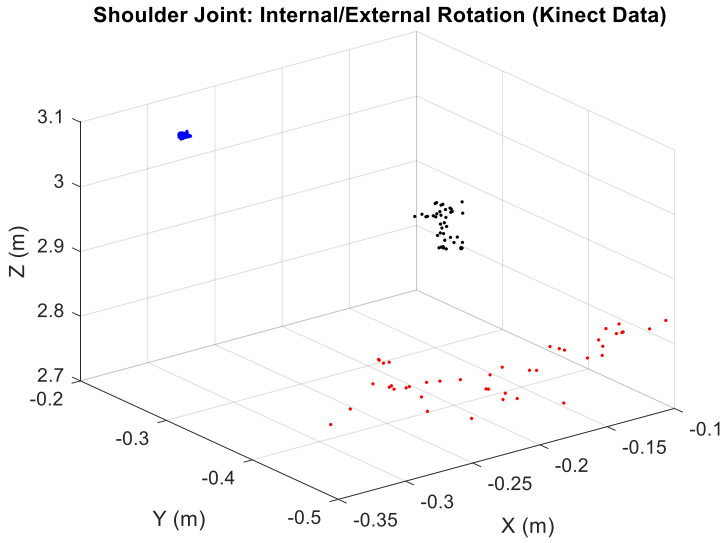

(a)

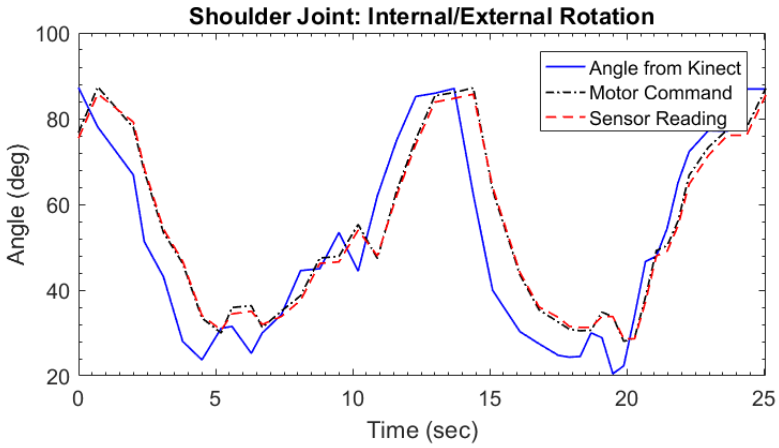

(b)

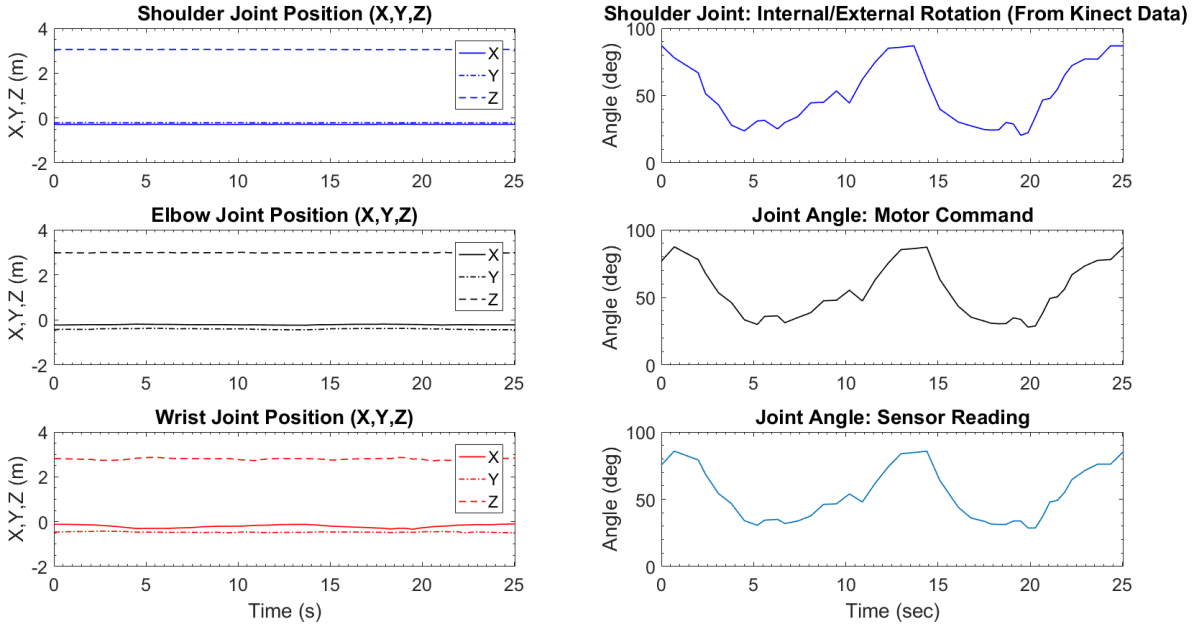

(c)

Figure 5.6 Shoulder joint internal/external rotation teleoperation. (a) Joint coordinate from Kinect (b) comparison between joint angles from Kinect and NAO robot.(c) coordinate data and joint angles from Kinect and NAO robot.

Figure 5.6 shows the hand position of NAO robot and human operator at different times of shoulder joint internal/external rotation motion. Motion start from 90 degree and end at 20 degree. Figure5.6

(a) and (c) shows the coordinate data obtained from Kinect sensor for shoulder, elbow and wrist joint .For shoulder internal/external rotation joint motion coordinates for elbow and shoulder joint form Kinect frame should be similar for all position because only wrist joint is moving here. In the Figure 5.6 (a) it is seen that all the blue and black points are clustered in same position throughout the time. Figure 5.6 (b) and (c) display the trajectory followed by human operator and NAO robot.

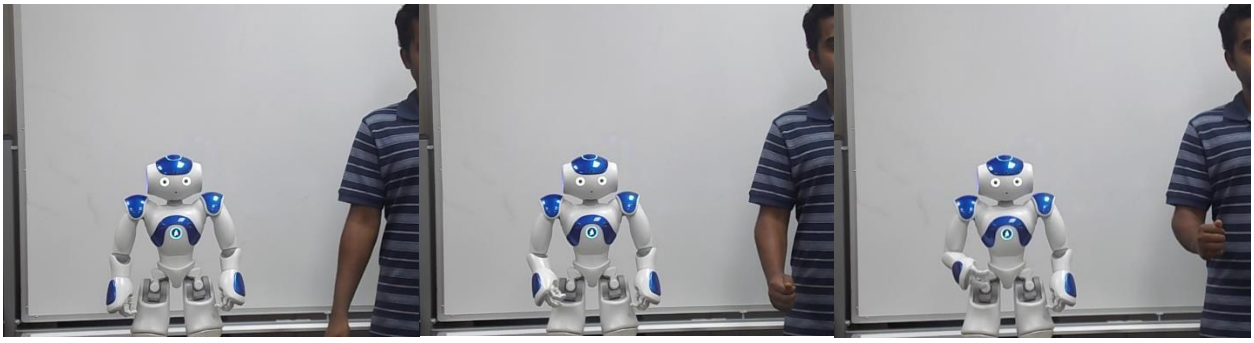

Figure 5.7 Arm position of human operator and NAO robot during elbow joint flexion/extension motion during teleoperation

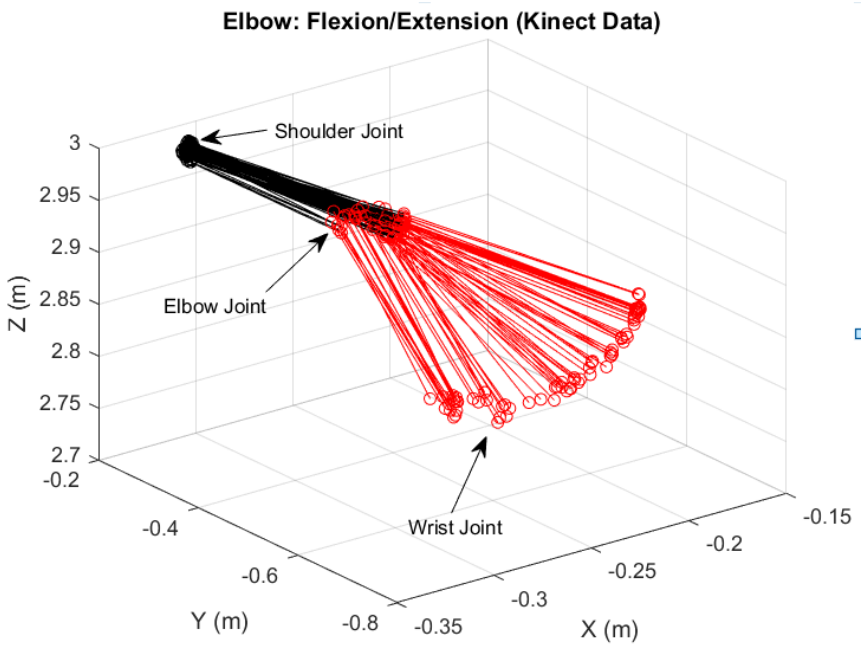

(a)

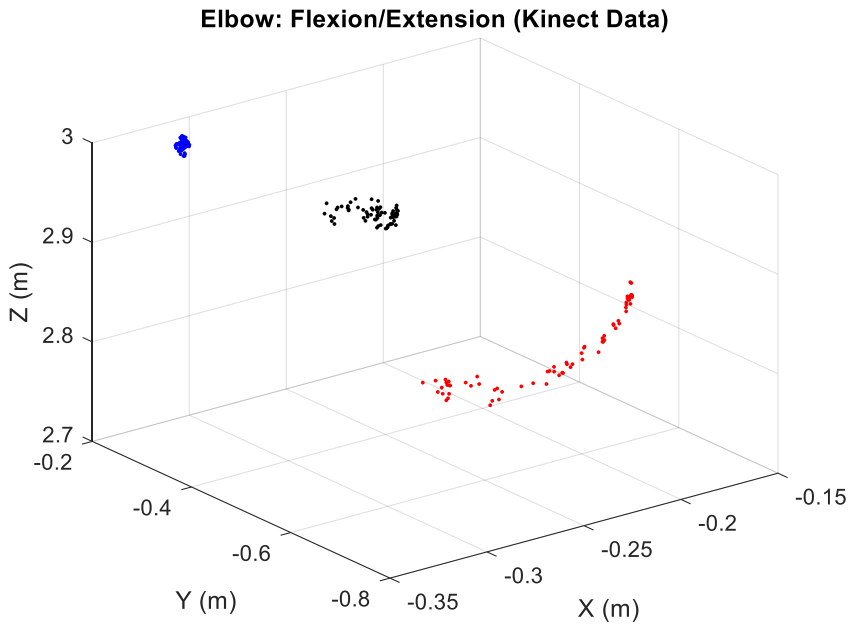
Elbow: Flexion/Extension (Kinect Data)
3
2.9
2.8
2.7
Z (m)
-0.2
-0.4
-0.6
-0.8
Y (m)
-0.35
-0.3
-0.25
-0.2
-0.15
X (m)

(b)

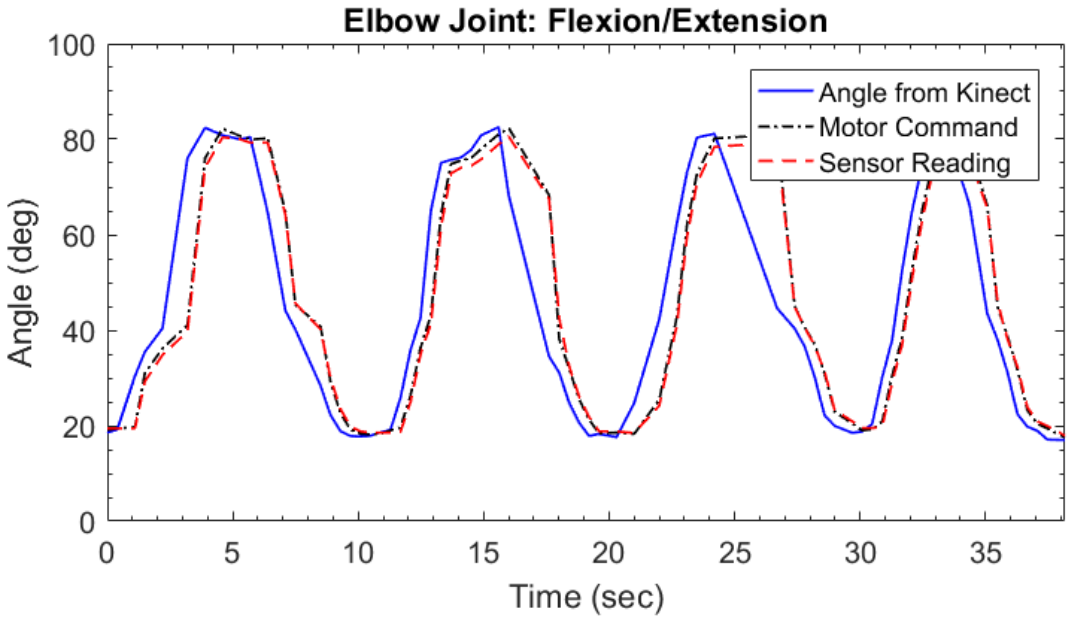
Elbow Joint: Flexion/Extension
Angle from Kinect
Motor Command
Sensor Reading
Angle (deg)
100
80
60
40
20
0
0
5
10
15
20
25
30
35
Time (sec)

(c)

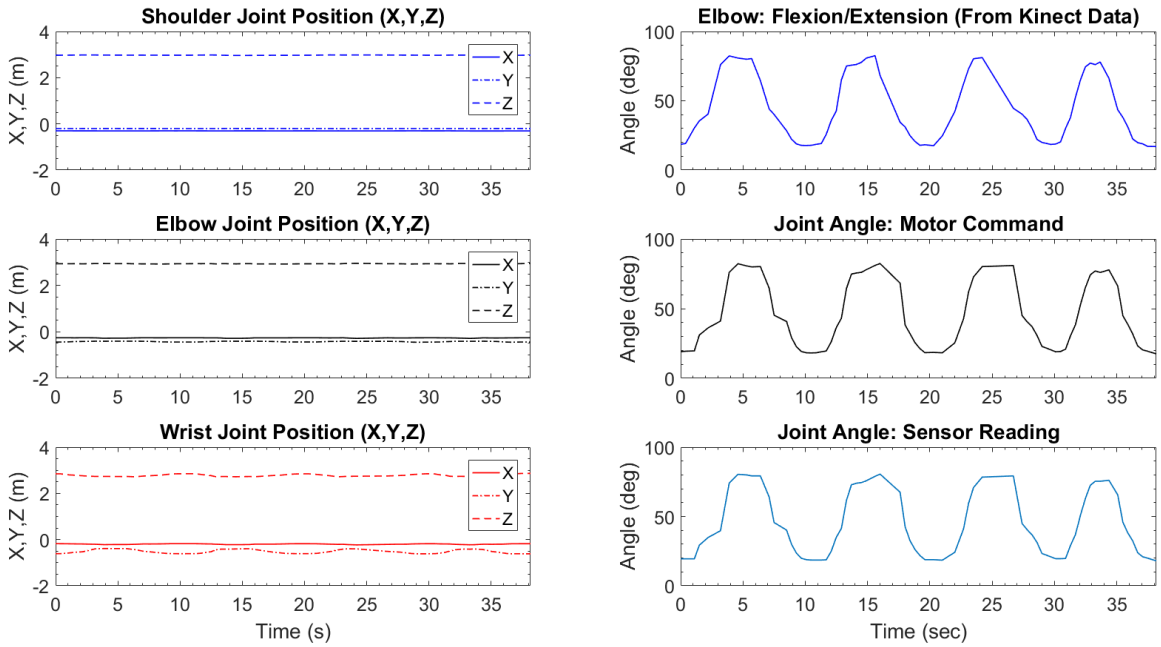

(d)

Figure 5.8 Elbow flexion/extension teleoperation. (a) Skeleton with joint coordinate from kinect(b) Joint coordinate from Kinect (c) comparison between joint angles from Kinect and NAO robot.(d) coordinate data and joint angles from Kinect and NAO robot.

Figure 5.8 shows the hand position of NAO robot and human operator at different times of elbow joint flexion/extension motion. Motion start from 15 degree and end at 85 degree. Figure 5.8 (a) (b) and (c) shows the coordinate data obtained from Kinect sensor for shoulder, elbow and wrist joint .For elbow flexion/extension motion joint coordinates for elbow and shoulder joint form Kinect frame should be similar for all position because only wrist joint is moving here. In addition, the X coordinate for wrist joint should constant as the potion is in YZ plane. Obtain result from Kinect so the same result. In the Figure 5.8 (b), it is seen that all the blue and black points are clustered in same position throughout the time. Figure 5.8,(b) and (c) display the trajectory followed by human operator and NAO robot.

Finally, we conduct experiment for multi joint movement. First multi joint experiment was shoulder joint horizontal flexion/extension. This motion is the combination of shoulder joint vertical flexion/extension and abduction/adduction. The obtained results are shown Figure 5.9 and Figure 5.10. Our second multi joint experiment was diagonal reaching which is a combination of three joint motion shoulder vertical flexion/extension and abduction/adduction and elbow flexion/extension the result for this experiment shown in Figure 5.11 and Figure 5.12

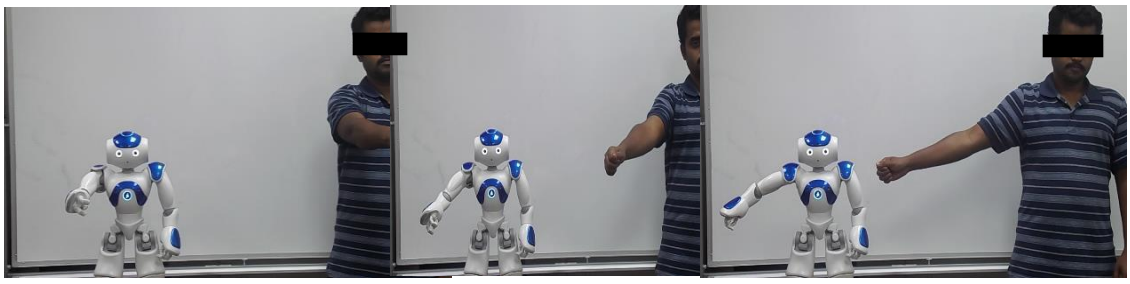

Figure 5.9 Arm position of human operator and NAO robot during Shoulder joint horizontal flexion/extension motion during teleoperation

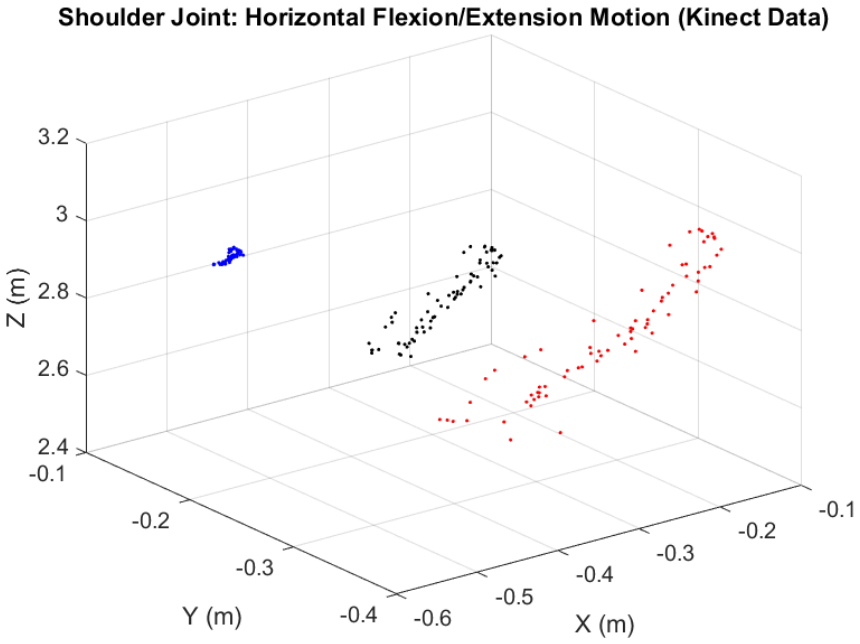

(a)

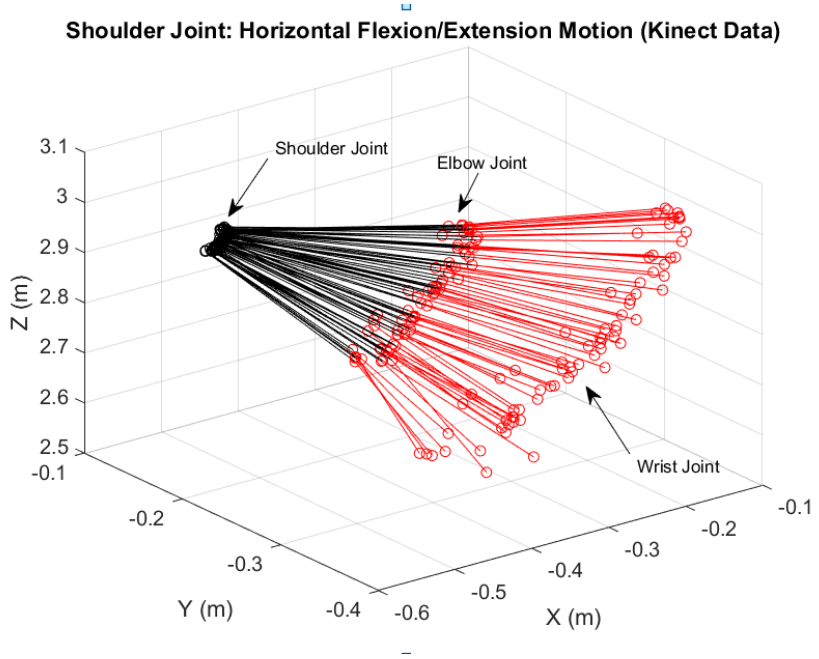

(b)

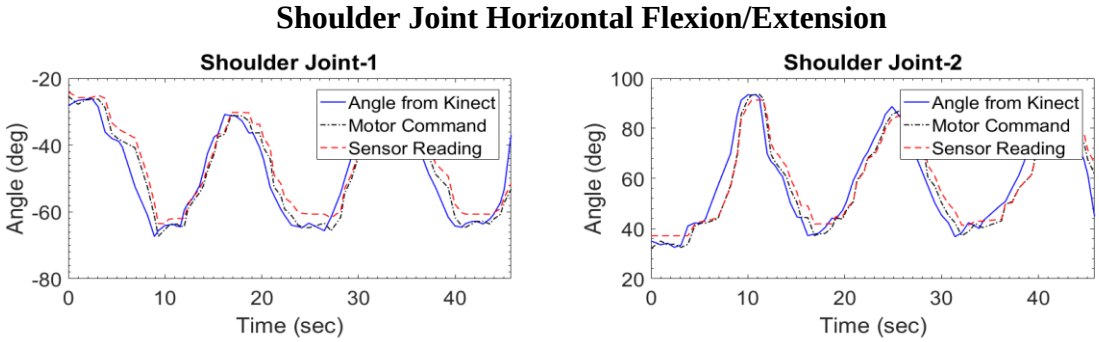

(c)

Figure 5.10 Shoulder joint horizontal flexion/extension teleoperation. (a) Joint coordinate from Kinect (b) skeleton with joint coordinate from Kinect (c) comparison between joint angles from Kinect and NAO robot.

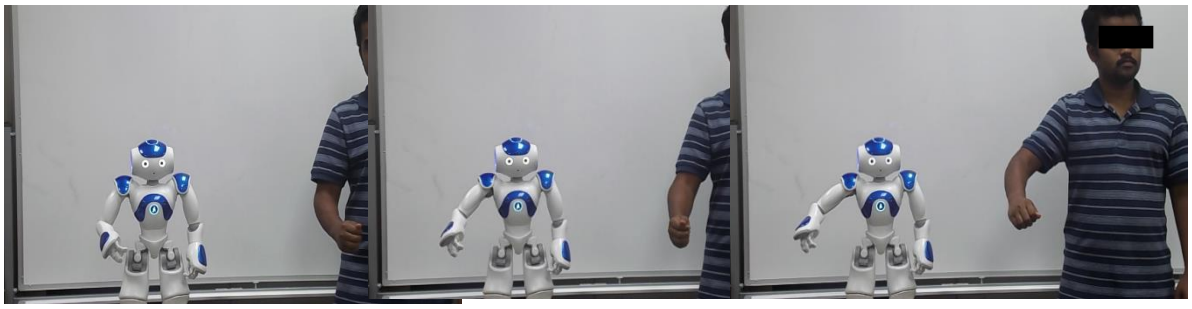

Figure 5.11 Arm position of human operator and NAO robot for Diagonal reaching motion during teleoperation

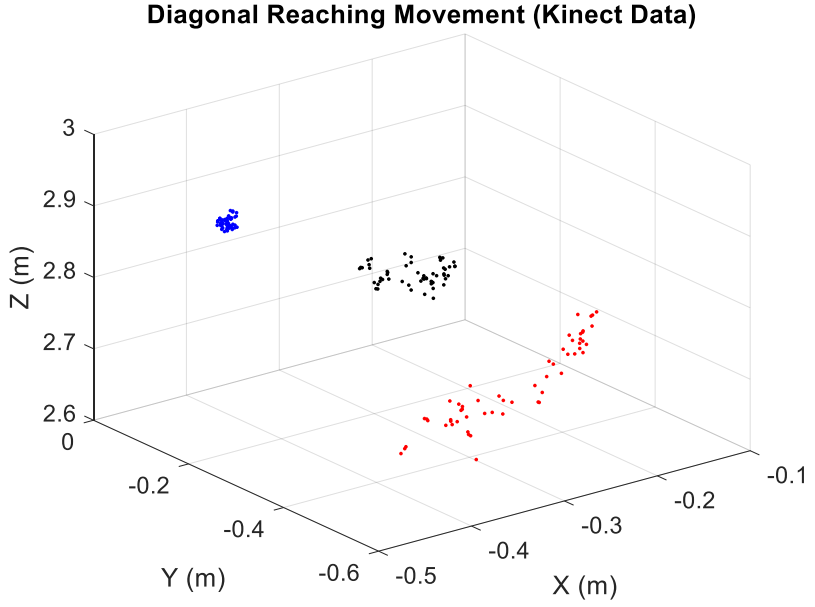

(a)

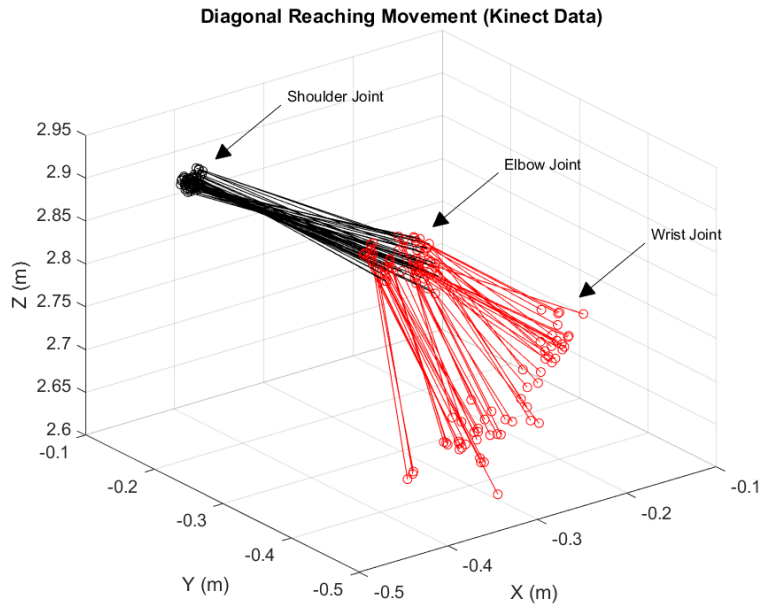

(b)

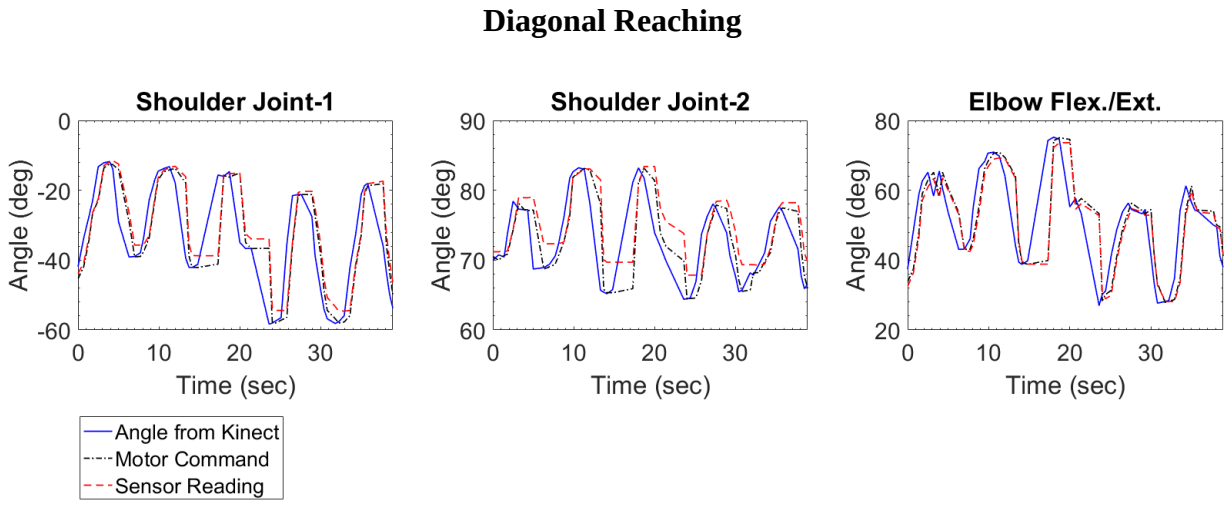

(c)

Figure 5.12 Diagonal reaching teleoperation. (a) Joint coordinate from Kinect (b) skeleton with joint coordinate from Kinect (c) comparison between joint angles from Kinect and NAO robot

From the result of all this experiments it is clear that there is a lagging exist between the human operator angle and that of NAO robot. However, the pattern of trajectory followed by the

NAO robot was exactly same that of the human operator. The main objective of teleoperation is to follow the motion trajectory produced by the human operator. Which is fulfilled in our case. By this method, one can easily control NAO robot joint angle remotely as long as they are connected to same network. It will be useful to introduce new exercise remotely.

CHAPTER 6

NAO GUIDED SUPERVISED REHABILITATION

This chapter focuses on Aim-3. To develop a supervision or an observation system of rehabilitation exercise using Kinect and humanoid robot NAO. In Aim-1, a set of rehabilitation exercises library have been built for NAO robot to demonstrate and instruct subject during rehabilitation. These are limited to instruction level only. There is no room for supervision or taking feedback from subject. Furthermore, in Aim-2 described in the previous chapter, teleoperation for remote rehabilitation has been introduced and that could introduce any new exercise remotely as well. Neither Aim-1 nor Aim-2 can be supervised by NAO robot. However, the ongoing chapter describes a system that uses Kinect to observe the exercise performed by subject in front of it has been developed. Based on this observation NAO provides feedback to the subject about his/her performance. First, we describe about supervision system then discuss about the experimental result in rest of this chapter.

6.1 Supervision system using NAO and Kinect

In this study, we only focused on the visual supervisions for the performed exercise in front of NAO robot. Here visual supervision means supervised all those facts that can be easily detected by normal vision. We considered following key points to be supervised:

- Accuracy of performed exercise
- Time required to perform the exercise
- Range of motion for a particular exercise.

First, the accuracy means the right way to perform a particular exercise. For instance, only shoulder joint θ_2 will vary when subject is asked to do shoulder vertical flexion/extension exercise in ideal case while not all other joints should be moving. If any other joints rotate, we term this not the right way to perform shoulder vertical flexion/extension exercise. Second, time required is quantified by the amount of time be taken by the subject to complete given exercise. With the feedback based on time being either okay, too fast, or too slow. Third, range of motion means the maximum angle covered during the given exercise.

To develop this supervision system we used Kinect sensor for smart vision and analyze the motion of the performed exercise. The Kinect acts as vision system for NAO robot and send the analyzed result to NAO robot that provides the feedback of how subject performed exercise eventually.

Supervision system is more like cooperative exercise described in chapter 5. The only difference is that in this case NAO examines the performed exercise through Kinect and provides feedback.

6.2 Performance analysis

We conducted individual joint motion exercise of three joint (shoulder abduction/adduction, shoulder vertical flexion/extension and elbow flexion extension/extension) and one multi joint motion exercise (diagonal reaching movement) to determine performance of the supervision system. In ideal case for a single joint motion, only that joint angle can vary and other are not supposed to move. However, human arm movements do not follow the ideal case and they are highly variable (Sanger 2000, Sarlegna and Sainburg 2007). That is why, for single joint

movement, we considered that other joint angle might change within a range. For other joint angle lying outside the range, the supervision system evaluates the performance as an inaccurate way. Every time when Kinect tracks a particular motion, MATLAB starts to track the time from beginning to finishing. When the exercise being performed is done, the maximum angle covered during the exercise is also calculated and all this feedback are sent to the NAO robot to give feedback to the subject.

Figure 6.1 shows the result of shoulder abduction/adduction motion done in correct way for three complete cycle. For shoulder abduction/adduction exercise, we considered the tolerable range for all other motion was ±20 degree from its initial position. The feedback provided for this exercise were the exercise is done perfectly for three complete cycle, has a maximum range during exercise of around 92 degree (value rounded to nearest integer), taking 26 seconds to complete the task.

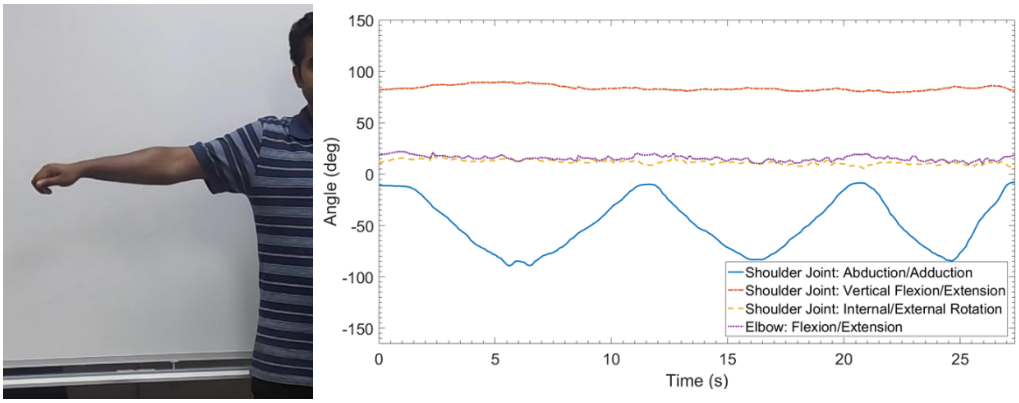

Figure 6.1performing shoulder abduction/ adduction motion in correct way.

In case of Figure 6.2 same task is performed but from the tracking angle it is clearly seen that the elbow joint crosses the range value. This shows that the experiment was not performed in

the right way. In that case, NAO provided a negative feedback and requested to repeat the task again.

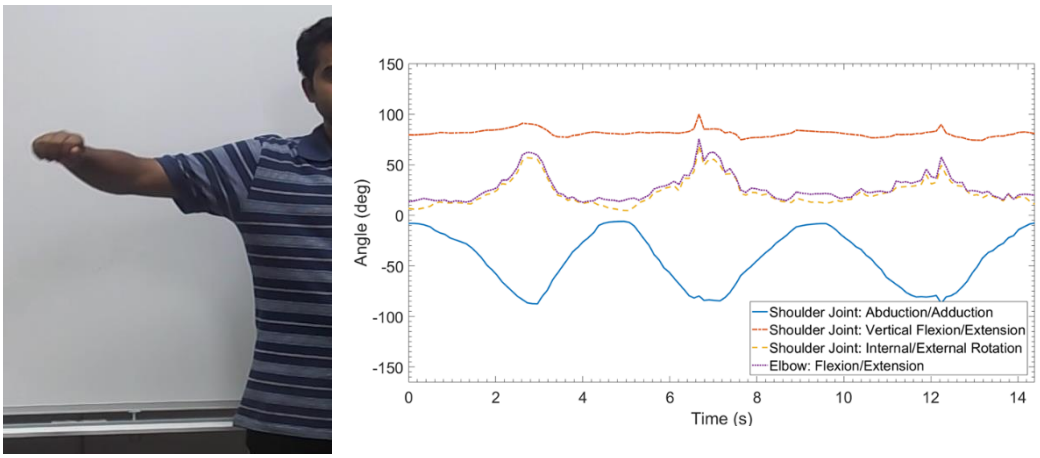

Figure 6.2 performing shoulder abduction/ adduction motion in inaccurate way.

For shoulder vertical flexion/extension motion, the tolerable range vary for each motion. The range for elbow flexion/extension and shoulder abduction/adduction was ±50 degree and for internal/external rotation, it was ±50 degree. Figure 6.3 shows the correct performance of this exercise, but in case of Figure 6.4, shoulder internal/external rotation cross the limit. Therefore, it is considered an inaccurate performance.

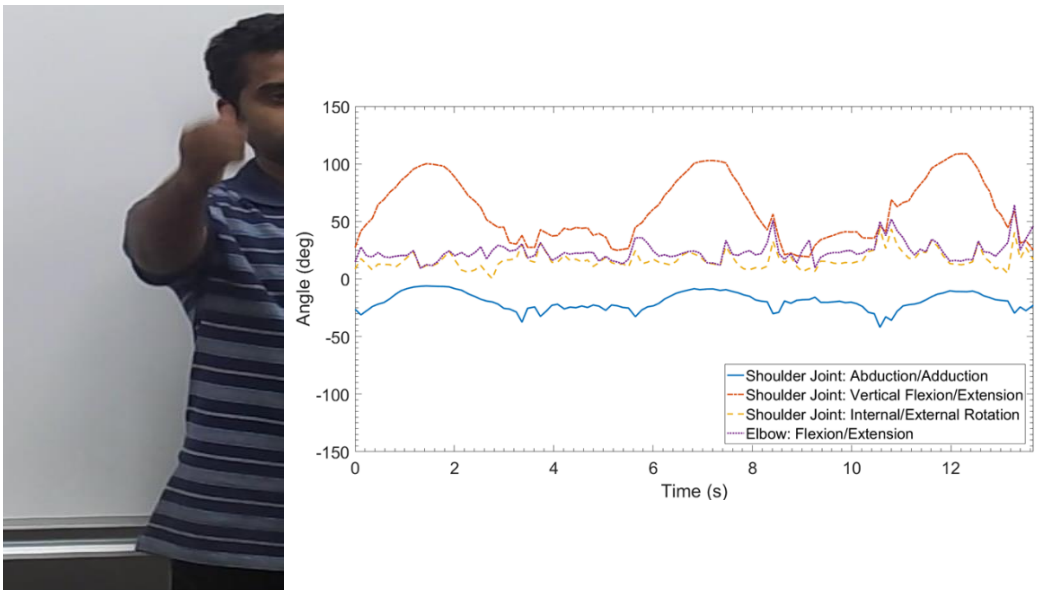

Figure 6.3 performing shoulder vertical flexion/extension motion in correct way.

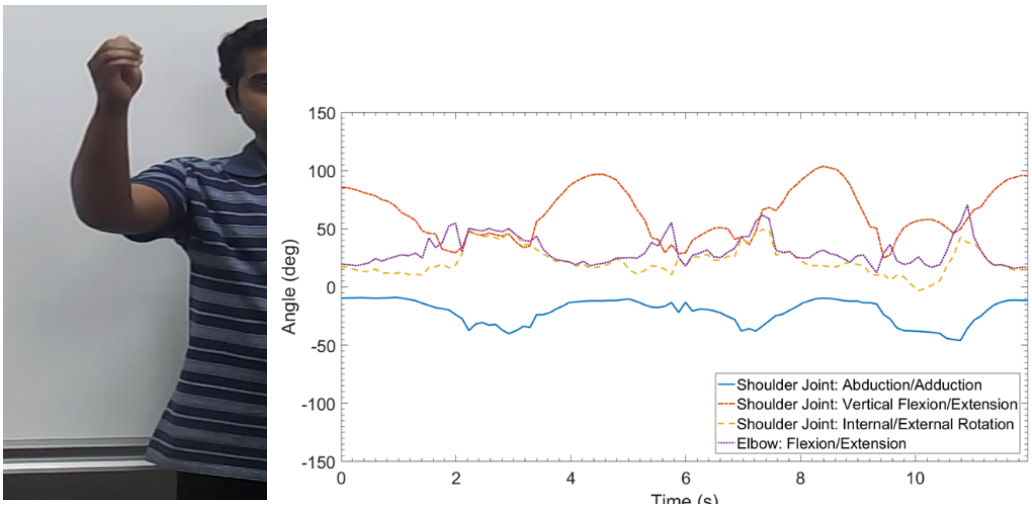

Figure 6.4 performing shoulder vertical flexion/extension motion in inaccurate way

Tolerable range for shoulder joint vertical flexion/extension choose varies largely because it is hard for Kinect to detect joint positon when two or more joint coincide to each other. Figure 6.5 illustrate a situation when wrist joint and elbow joint coincide each other. In this type of situation Kinect assume some random position for this two joint as result tracked joint fluctuated which also cause fluctuation in joint angle value. In case of shoulder vertical flexion/extension, this situation

happens several times which causes fluctuation in joint angles for elbow flexion/extension and shoulder abduction/adduction. To eliminate this effect we use a little bit of a large but tolerable range.

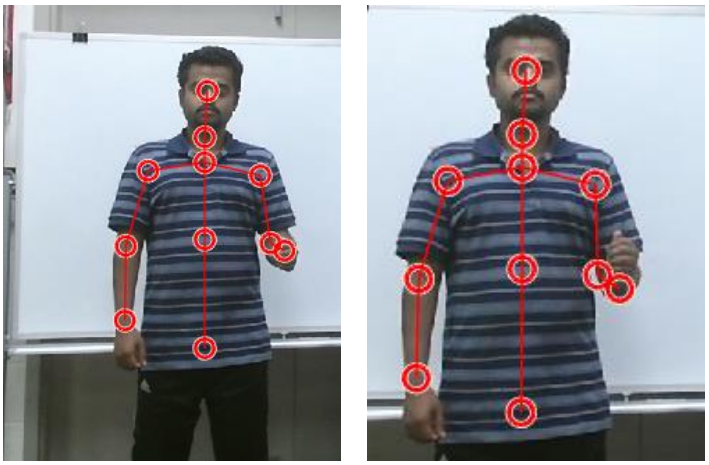

Figure 6.5 wrist and elbow joint tracked by Kinect sensor for same position.

Figure 6.6 shows the angle tracked for elbow flexion/extension exercise in correct way. Where the range for shoulder vertical flexion/ extension was ±35 degree, elbow internal/external rotation was ±50 degree and for shoulder abduction/adduction ±25 degree. Figure 6.7 shoulder joints are cross the limit.

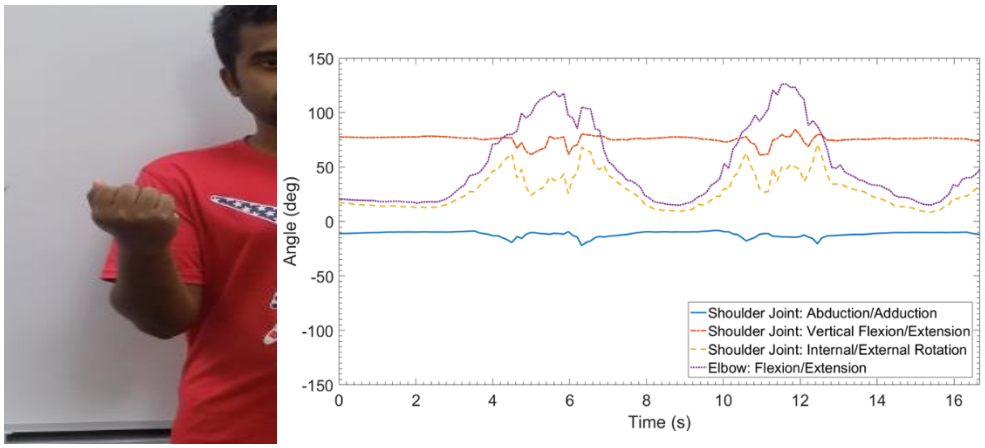

Figure 6.6 performing elbow flexion/extension motion in correct way

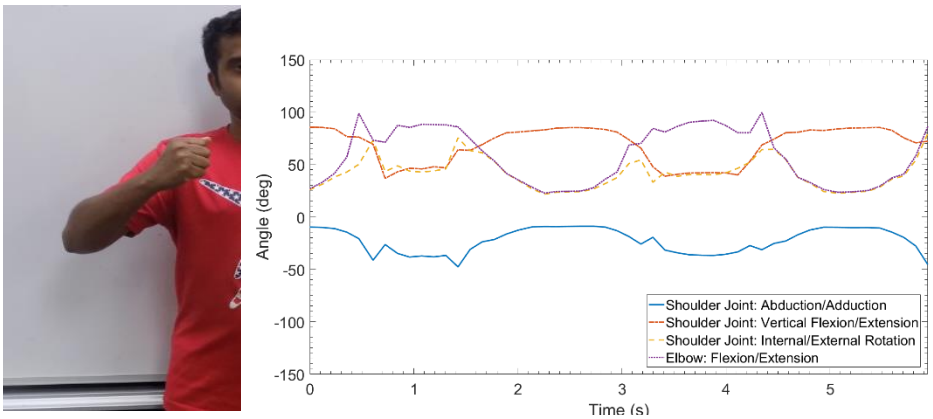

Figure 6.7 performing inaccurate elbow flexion/extension motion.

Figure 6.8 shows the angle tracking for performance analysis for diagonal reaching motion. In this motion in ideal case only three joint will be activate but in real case, all four motions are vary. Here the range of joint angle for each motion determined by experiment. The value will be vary for different types of disabilities.

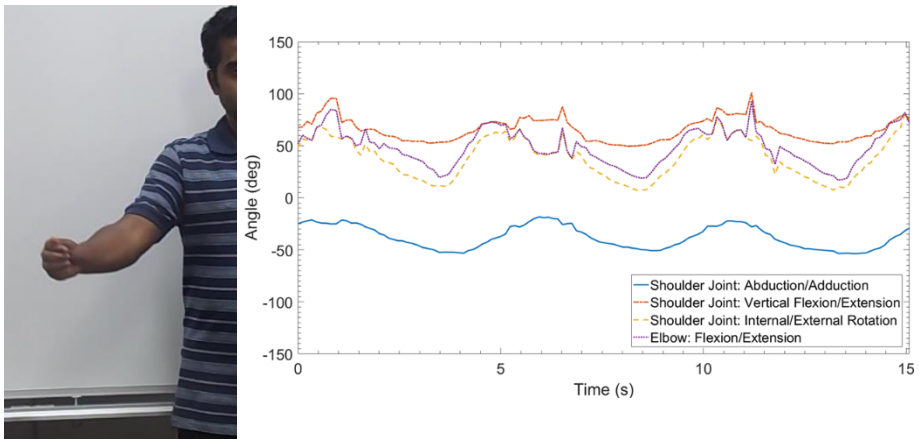

Figure 6.8 performing accurate diagonal reaching movement.

Conclusion:

Experimental results shown in sections 6.2 reveals that it is possible to develop a robot guided rehabilitation process only by tracking joint angles of human motion and NAO with Kinect sensor can be effectively used to develop a robot guided rehabilitation system.

CHAPTER 7

CONCLUSION AND FUTURE WORKS

8.1 Conclusion

A robot guided rehabilitation scheme was developed using a humanoid robot NAO and a Kinect sensor to provide grounds for effective rehabilitation of people with disabilities at the level of shoulder and elbow joint movements.

To demonstrate rehabilitation exercises with NAO, a library of recommended rehabilitation exercises involving shoulder and elbow joint movements was formed in Choregraphe (graphical programming interface). In experiments, NAO was maneuvered to instruct and demonstrate the exercises from the NRL. A complex 'touch and play' game was also developed where NAO plays with the subject that represents a multi-joint movements exercise.

To develop the proposed tele-rehabilitation scheme, kinematic model of human upper-extremity was developed based on modified Denavit-Hartenberg notations. A complete geometric solution was developed to find a unique inverse kinematic solution of human upper-extremity from the data obtained by Kinect. Experiments' results reveals that NAO can be tele-operated to instruct and demonstrate subjects to perform different arm movement exercises.

An intelligent control algorithm was developed in MATLAB for the proposed NAO guided supervised rehabilitation scheme. Experimental results show that NAO and Kinect sensor can effectively use to supervise and guide the subjects in performing active rehabilitation exercises for shoulder and elbow joint movements.

8.2 Future Works

To provide robot assisted rehabilitation future projects may include developing an intelligent robot sensor system that can assist therapist to instruct, supervise and demonstrate exercise intelligently. Future studies/works can also be expanded as follows:

- Developing a more reliable, cheap and noise free motion-tracking system because data form Kinect contains some noise.
- Developing a low cost humanoid robot with more processing power and high durability. NAO has limitations in his processing power.
- Develop a robot with more degree of freedom in its hand to cover all exercise for human upper limb rehabilitation exercise
- Introduce artificial intelligence in NAO to make it more cooperative in case of decision making.
- Introduce adaptive learning technology to NAO
- Develop a cloud server system of rehabilitation exercises in which individuals can access from anywhere to explore different types of rehabilitation exercises.

Finally, it is recommended to develop a rehabilitation protocol for robot-based rehabilitation

References:

Aldebaran http://doc.aldebaran.com/1-14/software/choregraphe/choregraphe_overview.html.

(2011, July 7, 2011). "Physical Therapy Standards." from http://www.brighamandwomens.org/Patients_Visitors/pcs/rehabilitationservices/StandardsofCare.aspx.

(2013). "NAOqi Framework." from http://doc.aldebaran.com/1-14/dev/naoqi/index.html.

Craig, J. J. (2005). Introduction to robotics : mechanics and control. Upper Saddle River, N.J., Pearson/Prentice Hall.

Denavit, J. and R. S. Hartenberg (1955). "A Kinematic Notation for Lower-Pair Mechanisms Based on Matrices." Trans ASME J. Appl. Mech. **23**: 215-221.

Garrec, P., J. P. Friconneau, Y. Measson and Y. Perrot (2008). ABLE, an innovative transparent exoskeleton for the upper-limb. 2008 IEEE/RSJ International Conference on Intelligent Robots and Systems, 22-26 Sept. 2008, Piscataway, NJ, USA, IEEE.

Gresham, G. E., D. Alexander, D. S. Bishop, C. Giuliani, G. Goldberg, A. Holland, M. Kelly-Hayes, R. T. Linn, E. J. Roth, W. B. Stason and C. A. Trombly (1997). "American Heart Association Prevention Conference. IV. Prevention and Rehabilitation of Stroke. Rehabilitation." Stroke **28**(7): 1522-1526.

Group, A. S. (2013). Aldebaran documentation.

Lum, P. S., C. G. Burgar and P. C. Shor (2004). "Evidence for improved muscle activation patterns after retraining of reaching movements with the MIME robotic system in subjects with post-stroke hemiparesis." IEEE Transactions on Neural Systems and Rehabilitation Engineering **12**(2): 186-194.

Mozaffarian, D., E. J. Benjamin, A. S. Go, D. K. Arnett, M. J. Blaha, M. Cushman, S. de Ferranti, J. P. Despres, H. J. Fullerton, V. J. Howard, M. D. Huffman, S. E. Judd, B. M. Kissela, D. T. Lackland, J. H. Lichtman, L. D. Lisabeth, S. Liu, R. H. Mackey, D. B. Matchar, D. K. McGuire, E. R. Mohler, 3rd, C. S. Moy, P. Muntner, M. E. Mussolino, K. Nasir, R. W. Neumar, G. Nichol, L. Palaniappan, D. K. Pandey, M. J. Reeves, C. J. Rodriguez, P. D. Sorlie, J. Stein, A. Towfighi, T. N. Turan, S. S. Virani, J. Z. Willey, D. Woo, R. W. Yeh and M. B. Turner (2015). "Heart disease and stroke statistics--2015 update: a report from the American Heart Association." Circulation **131**(4): e29-322.

Nef, T., M. Guidali, V. Klamroth-Marganska and R. Riener (2009). ARMin - Exoskeleton Robot for Stroke Rehabilitation. 11th International Congress of the IUPESM. Medical Physics and

Biomedical Engineering. World Congress 2009. Neuroengineering, Neural Systems, Rehabilitation and Prosthetics, 7-12 Sept. 2009, Berlin, Germany.

Rahman, M. H., K. Kiguchi, M. M. Rahman and M. Sasaki (2006). Robotic exoskeleton for rehabilitation and motion assist. 1st International Conference on Industrial and Information Systems, ICIIS 2006, August 8, 2006 - August 11, 2006, Peradeniya, Sri lanka.

Robotics, S. from https://www.ald.softbankrobotics.com/en/about-us.

Sanger, T. D. (2000). "Human arm movements described by a low-dimensional superposition of principal components." Journal of Neuroscience **20**(3): 1066-1072.

Sarlegna, F. R. and R. L. Sainburg (2007). "The effect of target modality on visual and proprioceptive contributions to the control of movement distance." Experimental Brain Research **176**(2): 267-280.

Terven, J. R. and D. M. Córdova-Esparza (2016). "Kin2. A Kinect 2 toolbox for MATLAB." Science of Computer Programming **130**: 97-106.

Truelsen, T., B. Piechowski-Jozwiak, R. Bonita, C. Mathers, J. Bogousslavsky and G. Boysen (2006). "Stroke incidence and prevalence in Europe: a review of available data." Eur J Neurol **13**(6): 581-598.

Wiki, i. (16 March 2014). "User Guide for Dual Depth Sensor Configuration." 2017, from http://wiki.ipisoft.com/User_Guide_for_Dual_Depth_Sensor_Configuration.

Winstein, C. J., A. S. Merians and K. J. Sullivan (1999). "Motor learning after unilateral brain damage." Neuropsychologia **37**(8): 975-987.

Winstein, C. J., J. P. Miller, S. Blanton, E. Taub, G. Uswatte, D. Morris, D. Nichols and S. Wolf (2003). "Methods for a multisite randomized trial to investigate the effect of constraint-induced movement therapy in improving upper extremity function among adults recovering from a cerebrovascular stroke." Neurorehabil Neural Repair **17**(3): 137-152.

World Health Organization. (2010). "Stroke, Cerebrovascular accident." Retrieved August 25, 2010, from http://www.who.int/topics/cerebrovascular_accident/en/.